Promoting Effect of nano Hydroxyapatite and Vitamin D3 on the Osteogenic Differentiation of Human Adipose-Derived Stem Cells in Polycaprolactone/Gelatin Scaffold for Bone Tissue Engineering

Mansoureh Sattary [1], Mohammad Rafienia [2], Mohammad Kazemi [3], Hossein Salehi [4]*, Mohammad Mahmoudzadeh [5]

1- Department of Biomedical Engineering, Science and Research Branch, Islamic Azad University, Tehran, Iran.

2- Biosensor Research Center, Isfahan University of Medical Sciences, 81744*176, Isfahan, Iran.

3- Department of Genetics, School of Medicine, Isfahan University of Medical Sciences, Isfahan, Iran.

4- Department of Anatomical Sciences and Molecular Biology, School of Medicine, Isfahan University of Medical Sciences, 81744*176, Isfahan, Iran.

5- Drug research program, Division of Pharmaceutical Biosciences, Faculty of Pharmacy, University of Helsinki, Viikinkaari 5E, P.O. Box 56, FI-00014 Helsinki, Finland.

* Corresponding author: Hossein Salehi

Email: ho_salehi@med.mui.ac.ir

ABSTRACT

Tissue engineering knowledge is a step toward the treatment of irreversible damages to human beings. In the present study, PCL/Gel, PCL/Gel/nHA, PCL/Gel/Vit D3 and PCL/Gel/nHA/Vit D3 (Polycaprolactone/Gelatin/Nanohydroxyapatite/Vitamin D3) composite scaffolds were successfully constructed using electrospinning method. The proliferation and differentiation of hADSCs into the bone phenotype were determined using MTT method, ALP activity, Von Kossa and Alizarin red staining, and qRT-PCR test. The simultaneous presence of nHA and vitamin D3 led to the increased activity of ALP in the early stages (on the 14th day) and increased mineralization in the late stages (on the 21th day) in differentiated hADSCs. Further, it was found that the use of nHA and vitamin D3 resulted in increased expression of BGLAP and COLL I and reduced expression of ALP and RUNX2 in hADSCs for 21 days. The results indicated that nHA and vitamin D3 have a synergistic effect on the osteogenic differentiation of hADSCs.

Keywords: Bone Tissue Engineering; HA nanoparticles; Vitamin D3; Human Adipose-Derived Mesenchymal Stem Cells; Osteogenic Differentiation.

[Graphical abstract]

1. INTRODUCTION

Craniofacial lesions occur due to trauma, periodontal disease, congenital and acquired defects, and bone respective surgery leads to decreased bone volume. This defect could not be restored naturally and requires an alternative bone graft. Autogenous bone graft is still considered as the gold standard for repairing such bone lesions. However, disadvantages of this method such as being limited as well as having painful surgery process and risk of infection, bleeding, nerve damage and loss of function have led researchers to seek an alternative method [1]. Tissue engineering, known as the knowledge of designing and constructing new tissue, emerged in the

early 90s in order to restore the function of defective organs or lost tissues. Principles of tissue engineering, cellular and molecular biologic expansion, and tissue formation are based on biological engineering. Perception of the function of cells and structure of the extracellular matrix, as well as sufficient knowledge about the construction of scaffolds to create an environment suitable for adhesion and maintenance of cells, are key concepts in tissue engineering. Bone tissue engineering necessarily requires three components: bone precursor cells, bone growth factor and a scaffold for adhesion and maintenance of cellular function [2].

New developments in the production of scaffolds as tissue substitutes are directed towards modeling of a natural extracellular matrix of tissues or substituted members. Production of scaffolds from nanofibers with natural extracellular matrix properties is more beneficial. At the start of the new century, many researchers have used electrospinning technique to produce nanofiber scaffolds. Electrospinning seems to be the only technique to manufacture continuous nanofibers at high rates. Thus, today, electrospinning process is widely used to produce nanofibers [3].

There are various natural and artificial polymers used in bone tissue engineering. Among them, polycaprolactone has many medical applications and is more suitable due to its compatibility with most drugs, cost-effective price and solubility in most organic solvents [4]. Yoshimoto et al., fabricated PCL fibrous scaffold using electrospinning technique and cultured rat mesenchymal stem cells (MSCs) on the scaffold [5]. The SEM images showed that the polymer-cell structure surface was covered with four layers of cells within four weeks. In addition, the mineral structure and collagen type 1 were observed during four weeks. They suggested that the electrospun PCL is a suitable candidate for bone tissue engineering applications [5]. But, the lack of bioactivity on these polymers is a problem due to lack cellular recognition sites [4].

Gelatin is a natural polymer derived from collagen throughout the hydrolysis process, which has a composition similar to that of collagen that is the main compound of ECM [6]. Gelatin has highly good adhesion, proliferation, and cellular differentiation properties; however, its low mechanical strength and high degradation rates have limited the use of this polymer in tissue engineering applications. Gelatin can improve PCL biodegradability for many bio applications and reduces the high cost of ultimate products. Therefore, with the proper combination of polycaprolactone and gelatin, one can overcome the critical constraints of both and improves the mechanical properties and degradation of the composition so that this compound becomes suitable for many biomedical applications [7].

In recent years, a number of researchers has emphasized the benefits of using nanocomposites in bone graft. The better performance of nanocomposites compared to integrated and conventional composites can be attributed to their similarity to the normal bone, which itself is a nanocomposite containing mainly HA nanocrystals and collagen nanofibers. Lary Hench., introduced polymer/apatite composite as the third generation of biomaterials, in which apatite crystals as nanorod (the apatite crystals contained in the bone are as elongated and directed particles) are parallel to the direction of the polymer fibers (preferably collagen) [8]. Wutti charoenmongkol et al., produced a new bone scaffold from a PCL solution containing hydroxyapatite nanoparticles using electrospinning method. They observed that the fiber diameter was increased by enhancing nanoparticle percentage or polymer solution concentration. Toxicity testing by osteoblasts has shown that these fibers are non-toxic and an appropriate candidate for bone repair applications. The presence of nanoparticles in PCL fibers increased the strength from 2.8 MPa to 3.6 - 3.9 MPa. They stated that increased fiber diameter due to the elevated percentage of nanoparticles is probably responsible for enhancing the observed strength [9]. In a

research, Yu et al., applied PCL/HA fibrous scaffold for bone reconstruction [10]. The use of HA increased the fiber wettability. Experiments showed that the increased adhesion of rat-derived osteoblasts on PCL/HA scaffold. The SEM images of the fibers immersed in simulated body fluid showed that the surface of the fibers was coated entirely with HA crystals after 7 days [10]. Research on nanostructured and nanoceramic biocomposites suggests that these materials are a good choice for bone tissue engineering applications and have improved biocompatibility and mechanical properties. The combination of polymer fibers and bioactive nanoparticles can be used to produce composite nanofibers [11]. Scaffold bioactivity stimulates cells towards osteogenesis and primary bone tissue formation [12]. Therefore, with the proper combination of polycaprolactone, gelatin and HA nanoparticles, it is possible to overcome the important constraints of all the three materials to make this compound suitable for many biomedical applications.

Vitamin D3, also known as calciferol, is one of the essential vitamins for the body and a fat-soluble vitamin, which helps bone growth and strength through the control of calcium and phosphorus balance. This vitamin helps the metabolism of bones by increasing the absorption of phosphorus and calcium from the intestines and reducing renal excretion. The shortage of this vitamin also causes osteoporosis in the old age [13]. Vitamin D3, from the biological aspects, greatly affects bone cells and contributes to the regulation of osteoblast and osteoclast activities that affect the bone synthesis, resorption, and regeneration processes. A prominent feature of vitamin D3 deficiency is the disruption of bone formation and mineralization [14]. Mason et al., showed that osteoblast precursors derived from human marrow (OPC1) can metabolize vitamin D precursors rapidly into active form of steroid ($1,25OH_2D_3$) and induce an osteogenic response. They showed that the use of vitamin D3 leads to increased alkaline phosphatase activity

associated with ECM maturation and calcium deposits. These findings provide a two-dimensional culture foundation for subsequent engineered tissue studies using the OPC1 cells [15]. Kato et al., reported a new method to purify the induced pluripotent stem (iPS)-derived osteoprogenitors (iPSop). They found that the use of vitamin D3 increased the expression of osteocalcin and reduced the expression of tissue-nonspecific alkaline phosphatase and RUNX2 in iPSop cells over a period of 14 days. Therefore, iPSop-day14 cells were promoted to mature osteoblasts by vitamin D3 treatment. In addition, they found that the vitamin D3 treatment for 14 days increased not only mineralization but also expression of osteocyte markers, including dentin matrix protein-1 and fibroblast growth factor-23, in iPSop cells. Therefore, vitamin D3 is a potent promoter for the osteoblast-osteocyte transition [13]. Similarly, Curtis et al., showed that the vitamin D3 is an essential factor in the differentiation of osteoblasts from human mesenchymal stem cells [16]. Song et al., investigated the effect of bone morphogenetic protein-2 (BMP-2) and vitamin D3 on the osteogenic differentiation of ADSCs. The osteogenic differentiation was assessed by staining and ALP activity, and mineralization were checked by Alizarin red staining. ALP activity and dose-dependent mineralization was increased in the early stages (ALP activity on day 7 and mineralization on day 14). As a result, BMP-2 and vitamin D3 promoted the osteogenic differentiation of ADSCs, which can act as synergism [17].

Most of studies in this field have been conducted on animal or human bone marrow-derived mesenchymal stem cells (BMSCs). However, unfortunately, the use of these types of cells has limitations that relate to the patient's discomfort and intolerance and the pain associated with bone marrow sampling. As an alternative, it has been suggested to use Human adipose tissue-derived stem cells (hADSCs) that are easily and painlessly extracted from the patient in large amounts. In addition, bone marrow extraction produces small amounts of cells and requires in

vitro culture. While adipose tissue is abundant and easy to achieve. Also, large amounts of hADSCs can be extracted from a small adipose tissue under local anesthesia [18].

In this research, the aim was to construct a PCL/Gel/nHA electrospun composite scaffold containing vitamin D3 to use in bone tissue engineering scaffolds. In addition, PCL/Gel/nHA/Vit D3 electrospun scaffold was used to culture hADSCs in vitro. The simultaneous effect of the use of HA nanoparticles and vitamin D3 on osteogenic differentiation of hADSCs and calcification of scaffolds was evaluated.

2. MATERIALS AND METHODS

2.1. Materials

Poly (ε-caprolactone) (PCL) (Mw = 80 kDa) was purchased by Sigma-Aldrich (St. Louis, MO). Gelatin (type B, from bovine skin) was provided from Merck (Darmstadt, Germany). Nano Hydroxyapatite (nHA) with average size 100 nm, was bought from Nick Seram Razi (Esfahan, Iran). Vitamin D3 was prepared from Zahravi Pharmaceutical (Tehran, Iran). Chloroform and acetic acid as a solvent were obtained from Merck and Sigma-Aldrich respectively. Methanol was purchased from Arman Sina Chemical & Pharmaceutical (Tehran, Iran). Deionized water was used in the experiment.

2.2. Electrospinning process

PCL (16% (w/v)) solution was solved in a mixture of chloroform/methanol (3:1 v/v). The solution was subjected to a magnetic stirrer for 4 hours at a speed of 600 rpm. Gelatin (8% (w/v)) solution was obtained using acetic acid (80 %v/v) by a magnetic stirrer at a speed of 500 rpm for 3 hours. After preparation of polymeric solutions, PCL and gelatin in volume ratio of (PCL/Gel) of 70:30 were mixed together and incubated for 72 h. After 72 h of incubation, gelatin solutions were uniformly dispersed in PCL solution [6]. Then, 20 wt% of HA nanoparticles was added to

PCL/Gel solution. For dispersing nanoparticles and preventing their agglomeration, the compound was then ultrasonically irradiated for 10 minutes. Afterward, the desired amount of vitamin D3 was added to the mixture and it was again stirred with the magnetic stirrer for 10 minutes until a solution with suitable viscosity was obtained. PCL/Gel, PCL/Gel/nHA, PCL/Gel/Vit D3 and PCL/Gel/nHA/Vit D3 scaffolds were prepared using electrospinning method. For electrospinning process, polymer composite solutions were filled in a plastic syringe (2 milliliters of each solution). Then, the fibers were collected on an aluminum foil of 15 cm × 15 cm × 1 mm. The spacing between the needle and the collector plate was adjusted to 13 cm, the solution injection rate to 1 ml/h and the supply voltage to 18 kV. After electrospinning, the scaffolds were kept in vacuum oven at 10 Pa pressure, 30 °C temperature and zero humidity for 24 hours to dry the fibers and completely remove the solvent from them. After drying, the scaffolds were easily removed from the aluminum foil.

2.3. SEM, EDX and TEM analysis

To investigate the morphology of the fibers, a scanning electron microscope (SEM) (Hitachi-S4160, Japan) was used. For this purpose, the samples were cut in 1 cm × 1 cm and coated with gold for 5 minutes. Imaging was carried out at 20 kV voltage and 1 mA current. Also, Image J software (National Institute of Health, USA) was used for measuring the diameter size of the fibers and the pore size, and MATLAB software was used to calculate the porosity percentage of the scaffolds [19]. Also, energy-dispersive x-ray spectroscopy (EDX Pegasus X4M) and X-ray map techniques were used to confirm the presence and distribution of nHA particles on the electrospun fibers. To study the internal structure and surface roughness of the fiber, the transmitted electron microscope (TEM, ZEISS, Germany), was used at a voltage of 100 kV.

2.4. Fourier Transform Infrared spectroscopy (FTIR)

Chemical analysis of PCL/Gel/nHA/Vit D3 fiber scaffold was performed by FTIR (IFS-66 V/S, Bruker, Ettlingen, Germany), over a wavenumber range of 400 and 4000 cm^{-1}.

2.5. In vitro drug release

Release of vitamin D3 from electrospun mats of PCL/Gel/nHA composite contains 2% and 5% Vit D3 was studied. In order to evaluate the release profile of PCL/Gel/nHA/Vit D3 composite, 10 mg of nanofiber were cut into specimens (15 mm × 15 mm) and were incubated at 37 °C in 5 mL of deionized water containing 1% ethanol (pH = 7.4) in a thermostatic shaker [14, 20]. The sample of 3 mL were periodically removed at predetermined time periods for quantification analyses and replaced by the same volume of fresh water/ethanol. The amount of released vitamin D3 was measured by UV–Vis (Shimadzu Europe -UV mini-1240). All measurements were performed in three replicates. Additionally, standard solutions were prepared through serial dilution of ethanol and vitamin D3 to plot the calibration curve of the concentration of vitamin D3 versus absorbance at $\lambda = 265$ nm ($R^2 = 0.9983$).

2.6. hADSCs isolation and expansion

Adipose tissue samples were obtained from the subcutaneous of young patients aged 20-40 years old, who underwent liposuction surgery in the hospital according to the surgeon's discretion, after receiving their consent. A 20-30 ml sample of adipose tissue was taken by a surgeon in the operating room and under sterile conditions. Adipose tissue sample, in the culture room and under the biological hood and sterile conditions, was chopped using a No. 22 scalpel blade. Then, the resulting fragments were washed several times with an antibiotic wash solution and its outer medium was removed [21, 22]. After transfer of the tissue to falcon, the 0.1% collagenase enzyme was added to the sample and then, the sample was placed in the incubator at 37 °C. After

0.5 hour passed, the solution was neutralized and removed by centrifugation. To the solution at the bottom of the tube, which are the extracted cells, DMEM (Dulbecco's Modified Eagle Medium; Bio Idea, India) with low glucose concentration containing 10% FBS (fetal bovine serum, Bio Idea, India) and 1% penicillin/streptomycin (Bio Idea, India) was added and then the cells were transferred to 75 cm^2 plastic tissue culture flasks. Twenty-four hours later, the cell culture medium was changed with a new medium. Every 2-3 days, the culture medium was replaced. The cells from passage 3-5 were used at this study.

2.7. Cell culture and seeding

The scaffolds prepared prior to culture were sterilized by placing in an ultraviolet chamber for 30 minutes. The cells were separated by Trypsin/EDTA (0.25% Trypsin in 0.04) from the flask surface. Then the cell suspension with specific concentration of 5×10^3 (cells/cm^2) was added to each scaffold in 24-well plates. In order to evaluate the osteogenic potential of the isolated cells, the culture medium cells was replaced with DMEM/Ham's Nutrient Mixture F-12 (DMEM/F-12 1: 1; Invitrogen) containing 5% FBS, 10 mM B-glycerol phosphate (Sigma; USA), 10 nM Dexamethasone (Sigma; USA) and 0.2 mM ascorbic acid 2-phosphate (Sigma; USA) and transferred to an incubator with 5% carbon dioxide at 37±1 °C [23]. Ten types of medium-based groups were prepared as follows (Table 1):

[Please insert Table 1 here]

2.8. Cell morphology study

To examine the adhesion and morphology of the cells, images of the cells were obtained by invert and scanning electron microscopy. To this end, the cells were seed at a concentration of 5×10^3 cells. After 1 and 7 days, cells were fixed with 4% glutaraldehyde solution. Subsequently, the

samples were dehydrated, each for 5 minutes, using 50, 70, 80, 90, 95 and 100% alcohols. Finally, the scaffolds were coated with gold and examined by SEM (Hitachi-S4160, Japan) [24].

2.9. MTT assay

To investigate the cell toxicity and proliferation, 3-(4,5-dimethyl-2-yl)-2,5-diphenyltetrazolium bromide (MTT) was used. The cell suspension at a concentration of 5×10^3 cells was cultured on the scaffolds. After 1, 4 and 7 days, the medium was removed from each well and the samples were washed with sterile PBS. Then, the medium containing 100 µl of MTT (0.5 mg/ml) was added to each 24-well plate. After 4 hours, the medium on the cells was removed and DMSO was added to dissolve generated purple formazan crystals. The concentration was then measured by a microplate reader (680, Bio-RAD) at a wavelength of 570 nm. A plate with higher optical density contains more cells [25].

2.10. Alkaline phosphatase (ALPase) activity assay

ALP enzyme belongs to the family of hydrolyzing enzymes, which is naturally found in all body tissues. This enzyme in most cells is in form of cell membrane enzymes, and its high concentrations have been so far reported in liver, kidney, bone (osteoblast). In the bone, this enzyme is involved in the process of bone matrix calcification and protein production along with the matrix. Therefore, during production of the bone matrix by osteoblasts, the activity of this enzyme is highly elevated and it is used as a characteristic factor to detect the activity of osteoblasts in the osteogenesis process [25]. ALP assay was performed using ALP assay kit (Pars Azmoon, Iran) according to the manufacturer's protocol on days 7, 14 and 21. Due to the presence of ALP in medium, p-nitrophenyl phosphate decomposed and converted to p-nitrophenyl. P-nitrophenyl produced a yellowish color, and this degradation reaction was eventually ended with the addition of 100 µl of 1N NaOH solution. In the last step, the

absorbance of the reaction product was evaluated using a microplate reader at the 405 nm wavelength [26].

2.11. Von Kossa staining

In order to assess the presence of inorganic matrix within the scaffolds using the invert microscopy, after 7, 14 and 21 days of culture of the cells on the scaffolds, they were first washed three times with distilled water and placed in silver nitrate solution (1%) under intense light for three hours. Then, silver nitrate solution was removed and the scaffolds were washed again three times with distilled water. By adding sodium thiosulfate solution (5%) for 5 minutes, unreacted silver was removed from the scaffolds. Finally, the scaffolds were washed with distilled water and observed by invert microscopy [27].

2.12. Alizarin red S histochemical staining

Alizarin red is used in biochemical tests to determine and measure the presence of calcium precipitation by osteogenic cells. Alizarin red can be used in the mineralization stages of extracellular matrix, during which extracellular matrix, like the actual bone, is calcined [26]. Alizarin red was used to detect mineralization on days 7, 14 and 21. Briefly, the scaffolds were washed several times with distilled water. The process of fixing the cell-scaffold structures was performed with a 4% paraformaldehyde for 15 minutes. Then, the scaffolds were washed again by distilled water. In the next stage, the cells were placed at room temperature in the presence of a 2% Alizarin red solution (pH= 4.1-4.3) for 45 minutes. At the end, the cells were washed twice with distilled water, and the stained mineral components were observed by an invert microscope. Quantitative measurement of amount of calcium precipitation was obtained by washing the scaffolds with acetone and xylene, solubilizing the red matrix precipitate in 10% cetylpyridinium

chloride, and reading the optical density of the solution [27].

2.13. Real-time quantitative (qRT-PCR)

Cell suspension at 2×10^4 cells/cm^2 concentration was added to the scaffolds and the culture plates were incubated 37±1 °C and 5% CO_2 for 21 days. The gene expression of COLL I, ALP, BGLAP, and RUNX2 were investigated by real-time PCR [28]. Total RNA was extracted by RNeasy Mini Kit (Qiagen, Valencia, CA) according to the manufacturer's instructions. The RNA was reverse transcribed using RevertAid First Strand cDNA Synthesis Kit (Thermo Scientific) with oligo dT primers. The real-time polymerase chain reaction was performed using BIOFACT™ 2X Real-Time PCR Master Mix kit (Biofact) and the StepOne Plus™ Real-time PCR Detection System (Applied Biosystems). Primer sequences are shown in Table 2. PCR reactions were carried out in a total volume of 20 µl. The PCR amplification conditions consisted of 15 min at 95 ºC followed by 40 cycles of denaturation step at 95 ºC for 15 sec and annealing and extension for 1 min at 60 ºC. The gene of interest was normalized against the reference gene glyceraldehydes-3-phosphate dehydrogenase (GAPDH). The expression level of each target gene was calculated by $2^{-\Delta\Delta CT}$. These experiments were carried out in triplicate and independently repeated at least three times.

[Please insert Table 2 here]

2.14. Statistical analysis

One-way ANOVA followed by Tukey's test was used for analysis of the significant difference at $P < 0.05$ between the obtained data. Experimental results were presented as mean ± standard deviation.

3. RESULTS

3.1. Scaffolds morphology

PCL/Gel, PCL/Gel/nHA, PCL/Gel/Vit D3 and PCL/Gel/nHA/Vit D3 fibers were prepared by electrospinning method. The parameters of applied voltage, space between needle and collector, polymer solution flow rate and polymer ratio in solution were used to produce smooth and bead-free fibers. Voltage at 18 kV, polymer solution flow rate at 1 ml/h, space between needle to collector of 13 cm, and mixed PCL/Gel with the ratio of 70:30 were the optimized parameters used in this study. Table 3 and Figure 1 show fiber properties and SEM images of composite scaffolds, respectively.

[Please insert Table 3 here]

As shown in Figure 1 and Table 3, all of the fibers were made in a relatively uniform size, with a mean diameter of 594, 631, 597 and 622 nm for PCL/Gel, PCL/Gel/nHA, PCL/Gel/Vit D3 and PCL/Gel/nHA/Vit D3, respectively. Adding nHA particles increased the fibers diameter size of PCL/Gel scaffold from 594 to 631 nm. But, by adding 2% Vit D3 (according to "3.3. Drug release study" section) to PCL/Gel composite scaffold, no significant change in fiber diameter size was observable. On the other hand, the simultaneous presence of nHA and vitamin D3 increased the diameter size of PCL/Gel composite scaffold fiber from 594 to 622 nm. The mean porosity percentage and pore size of PCL/Gel/nHA/Vit D3 composite scaffold were observed to be about 83.11% and 8.54 μm.

[Please insert Figure 1 here]

The EDX spectrum (Figure 2a) shows Calcium (Ca) and Phosphor (P) peaks with Ca/P = 1.68 (major components of HA), which confirms the presence of hydroxyapatite particles in PCL/Gel/nHA/Vit D3 composite. The electron map image in Figure 2b shows the distribution of

oxygen, calcium and phosphorus elements in PCL/Gel/nHA/Vit D3 composite scaffold which confirms that nHA particles are distributed uniformly throughout the fiber matrix.

[Please insert Figure 2 here]

The TEM image of PCL/Gel/nHA/Vit D3 composite scaffold is presented in Figure 3. As can be seen, TEM has shown an almost flat surface of this fiber. Also, the results of TEM image show that nHA particles have a size range of 60 - 100 nm.

[Please insert Figure 3 here]

3.2. Chemical analysis of scaffolds

The results of FTIR chemical analysis to describe the functional groups in PCL/Gel/nHA/Vit D3 composite fiber are presented in Figure 4. PCL-specific FTIR spectrum showed the peaks of 2931 cm^{-1} (asymmetric CH_2 stretching), 2858 cm^{-1} (symmetric CH_2 stretching), 1722 cm^{-1} (C=O carbonyl stretching), 1292 cm^{-1} (C-O and C-C stretching in crystalline phases), 1239 cm^{-1} (asymmetric C-O-C stretching) and peak 1161 cm^{-1} (symmetric C-O-C stretching) [29]. The FTIR spectroscopy of gelatin exhibited several characteristic bonds at 3433, 1653, 1543 and 559 cm^{-1}, respectively, belonging to corresponding stretching vibration of N-H (amide A), stretching vibration of C-O bond (amide I), due to coupling of bending of N-H bond and stretching of C-N bond (amide II) and N-H [6]. Two strong bonds at 1722 and 1292 cm^{-1} in FTIR spectrum of PCL/Gel composite scaffold belong to the main PCL characteristic bonds. On the other hand, the characteristic bonds of gelatin amide appeared in 1653 cm^{-1} (amide I) and 1543 cm^{-1} (amide II) with less sharpness and were visible at 1651 and 1542 cm^{-1}, respectively. The only difference between PCL and PCL/Gel bonds is the appearance of the amide group in PCL/Gel spectrum, which confirms the presence of gelatin in PCL fibers after combining two polymers and their electrospinning. The FTIR spectrum of HA nanoparticles shows five important bonds at 570 and

601 cm^{-1} (belonging to υ_4 $P0_4$), 631 cm^{-1} (belonging to free OH ion-bonded hydrogen), 1041 cm^{-1} (corresponding to υ_3 PO_4) and 3572 cm^{-1} (belonging to OH ion-bonded hydrogen stretching) [30]. The FTIR spectrum of PCL/Gel/nHA scaffold revealed all the characteristic bonds of PCL/Gel and nHA. The peaks of 570, 601 and 1041 cm-1 belonging to PO4 group of hydroxyapatite were seen in PCL/Gel/nHA scaffold, but not present in PCL/Gel scaffold. On the other hand, PCL/Gel/nHA FTIR spectrum showed the characteristic bonds of amide gelatin at 1651 (amide I) and 1542 cm-1 (amide II), and two peaks belonging to C=O and C-O groups of PCL at 1292 and 1722 cm-1, respectively. According to results obtained by Urankar and Toyran, vitamin D3 FTIR spectroscopy had several characteristic bonds at 3300, 2940, 2850, 1650 and 1450 cm^{-1} [31, 32]. The only difference between PCL/Gel/nHA and PCL/Gel/nHA/Vit D3 bonds is the appearance of an asymmetric CH3 stretching at 2939 cm-1 in PCL/Gel/nHA/Vit D3 spectrum, which confirms the presence of vitamins D3 in PCL/Gel/nHA/Vit D3 composite scaffold after combining components and their electrospinning. On the other hand, C-H stretching bond at 2858 cm^{-1} and C-H bending bond at 1447 cm^{-1} overlap with PCL characteristic bonds, which are difficult to differentiate. The peaks at 1651 cm^{-1} and in the range of 3300 to 3500 cm^{-1} were assigned to water, which is stronger due to the hydrophobic nature of vitamin D3 in PCL/Gel/nHA. Therefore, according to the results, the presence of vitamin D3 was confirmed in PCL/Gel/nHA/Vit D3 composite scaffold.

[Please insert Figure 4 here]

3.3. Drug release study

The cumulative release profiles of vitamin D3 from electrospun PCL/Gel/nHA/Vit D3 fibers in water/ethanol at 37 °C within 30 days are shown in Figure 5. In PCL/Gel/nHA scaffold containing 2% vitamin D3, the amount of drug release over the first day was observed to be very

minimal and then gradually increased afterwards (Figure released vitamin D3 in this scaffold was found to be 34%. The release kinetics of PCL/Gel/nHA scaffold containing 5% vitamin D3 can be shown in two stages, in the first phase, exhibited a burst effect release of about 40% at the first day. Then, in the second release phase, the remaining of the loaded drug was released over 30 days. Since a significant prerequisite for the successful designing of a drug delivery system for bone tissue engineering is the slow release of the drug over several weeks to sustain optimal therapeutic concentrations [20], we decided to limit our experiments to 2% drug loading.

[Please insert Figure 5 here]

3.4. Cell culture

Fibroblast-like morphology of cultured stem cells was observed by invert microscope (Figure 6). These cells were characterized in our previous study [33]. In the third passage, a uniform population of spindle-shaped cells with distinct nuclei was observed. To assess osteogenic differentiation, hADSCs in the passages 3 to 5 were used.

[Please insert Figure 6 here]

3.5. Cell proliferation

This test was performed to evaluate the toxicity and proliferation of cells on the scaffolds. The quantitative analysis diagram of cell proliferation (Figure 7) shows that the proliferation of cells on the first day after culture did not change significantly for the scaffolds compared to the control sample (PCL/Gel was selected as control sample) ($P>0.05$). All samples were normalized to PCL/Gel sample. On the fourth day after culture, increased proliferation and survival of the cells on all the scaffolds can be clearly observed compared to the control sample. Also, the rate cell

viability in PCL/Gel/nHA/Vit D3 scaffold on the sev

increase compared to that in the other scaffolds ($P < 0.05$). It should be noted that for cell culture testing, bone induction medium was used.

[Please insert Figure 7 here]

3.6. Cell Adhesion and Morphology

The images in Figure 8 show scanning electron microscopic images of the proliferation and adhesion of hADSCs cultured on the scaffolds in 1 and 7 days after culture. As seen in these images, after 24 hours, the cells interacted with each other in PCL/Gel/nHA, PCL/Gel/Vit D3 and PCL/Gel/nHA/Vit D3 scaffolds and proliferated. By comparing the microscopic images in Figure 8, an increased cell proliferation in these three composite scaffolds compared to the pure PCL/Gel scaffold was observable, and these scaffolds indicated good biocompatibility as well as good and normal adhesion and expansion both on the days 1 and 7 after culture.

[Please insert Figure 8 here]

3.7. Osteogenic differentiation of hADSCs on the scaffolds

ALP activity of differentiated hADSCs on the composite scaffolds on the days 7, 14 and 21 after culture is shown in Figure 9. According to this Figure, ALP activity was not significantly different between the scaffolds on the day 7 ($P>0.05$). On the 14th day, however, significant ALP activity was observed in PCL/Gel/nHA, PCL/Gel/Vit D3 and PCL/Gel/nHA/Vit D3 scaffolds compared to PCL/Gel scaffold ($P < 0.05$). Also, the results of the 14th day showed a significant difference in the activity of ALP between PCL/Gel/nHA/Vit D3 scaffolds compared to PCL/Gel/nHA and PCL/Gel/Vit D3 scaffolds ($P < 0.05$). As shown in Figure 9, ALP activity of the scaffold groups was associated with a decrease on the 21st day.

[Please insert Figure 9 here]

3.8. Mineralization

To evaluate the mineral content of the matrix, calcium content of the scaffolds was evaluated by Alizarin red and Von Kossa staining in 7, 14 and 21 days after culture.

The results of Von Kossa staining on PCL/Gel, PCL/Gel/nHA, PCL/Gel/Vit D3 and PCL/Gel/nHA/Vit D3 scaffolds are shown in Figure 10. The presence of dark colored deposits indicates the inorganic matrix produced by stem cells cultured on PCL/Gel/nHA, PCL/Gel/Vit D3, and PCL/Gel/nHA/Vit D3 scaffolds. As seen from the invert microscopic images, scaffolds containing HA nanoparticles and vitamin D3 exhibit highest amount of mineral deposits compared to the other scaffolds. On the other hand, the pure PCL/Gel scaffold did not show any deposition on either of the days 7 and 21.

[Please insert Figure 10 here]

Figure 11 shows the images of the scaffolds after staining of Alizarin red. The staining of the mineral deposits in PCL/Gel scaffold was similar to each other on the day 7, 14 and 21, and no red deposition was observed in this scaffold. After 14 days, Alizarin red staining of the scaffolds confirmed the presence of mineralization in PCL/Gel/nHA, PCL/Gel/Vit D3 and PCL/Gel/nHA/Vit D3 scaffolds. Over time, mineral deposition in PCL/Gel/nHA, PCL/Gel/Vit D3, and PCL/Gel/nHA/Vit D3 scaffolds increased, which peaked on the 21st day. The staining of mineral deposits 21 days after culture shows that the amount of mineral deposits in PCL/Gel/nHA/Vit D3 scaffold matrix was more than that in PCL/Gel/nHA and PCL/Gel/Vit D3 scaffolds in the same period. Moreover, the semi-quantitative analysis performed by extraction of Alizarin red spots (Figure 12) shows that the production rate of the matrix mineralized in PCL/Gel/nHA/Vit D3 scaffold was significantly higher on the 21st day ($P < 0.05$) and had a

statistical significant difference compared to PCL/Gel/nHA and PCL/Gel/Vit D3 scaffold ($P < 0.05$).

[Please insert Figure 11 here]

[Please insert Figure 12 here]

3.10. Expression of osteogenic markers

Real time-PCR was used to evaluate the osteogenic genes expression of differentiated stem cells on the scaffolds. Four genotypes of COLL I, ALP, RUNX2, and BGLAP were evaluated in the study of gene expression. The results of cell gene expression analysis in the prepared scaffolds are shown in Figures 13 and 14. As can be seen in Figure 13, mRNA expression level in COLL I, BGLAP, ALP and RUNX2 increased significantly in all the scaffolds ($P < 0.05$) when culture was carried out in the bone induction medium, as compared to the cell culture medium. On the other hand, among the scaffold groups, there was a superior expression in PCL/Gel/nHA/Vit D3 scaffold. COLL I, known as an early marker of osteoprogenitor cells, has upregulated in scaffold groups compared to control group (Figure 14). BGLAP, which appears as a late marker of osteoblast development with the matrix mineralization, is maximally expressed on the day 21 (Figure 14). The level of ALP expression has been reduced on the 21st day, during the mineralization phase (Figure 14). Relative expression of RUNX2, a key factor in bone transcription, also decreased on the 21st day (Figure 14). According to Figure 14, on the 21st day after cell culturing, all four COLL I, BGLAP, ALP and RUNX2 genes were expressed, but COLL I and BGLAP had the most pronounced expression in all groups. That's while, ALP and RUNX2 exhibited lower expression levels than COLL I and BGLAP in the same period (Figure 14). Regarding the semi-quantitative RT-PCR analysis, the expression levels of COLL I,

BGLAP, ALP and RUNX2 in the cells cultured on PCL/Gel/nHA/Vit D3 scaffold significantly increased, as compared with the other scaffolds ($P < 0.05$).

[Please insert Figure 13 here]

[Please insert Figure 14 here]

4. DISCUSSION

Tissue engineering is the use of biological and engineering sciences to biologically regenerate or substitute damaged organs and lost tissues [2]. There are many methods for the production of three-dimensional scaffolds, and electrospinning has been widely considered recently among all due to its ease of use, production of very thin polymer fibers, high specific surface area and high modifiability [3]. Among the various polymer composites, the combination of gelatin and polycaprolactone has received the most attention. Polycaprolactone (a synthesized, hydrophobic, and flexible polymer with a low degradation rate) [4] and gelatin (a natural, hydrophilic, abundant polymer with a high degradation rate) blends are interesting because their components have completely different structures and features [6]. Research on nanostructured and nanoceramic (such as nHA) biocomposites suggests that these materials are a good choice for bone tissue engineering applications and have improved biocompatibility and mechanical properties. The combination of polymer nanofibers and bioactive nanoparticles can be used to produce composite nanofibers [9-11].

Vitamin D3 has a wide range of physiological functions in the body, most important of which is to maintain calcium and phosphorus balance. Although it has been reported in a study on mice [13] that treatment with vitamin D3 improves the initial stages of osteoblast differentiation in

vitro, other in vitro studies have shown that vitamin D3 induces expression of specific bone markers in stages of osteoblast differentiation [14-17].

Mesenchymal stem cells can be used as a suitable cellular source for reconstructive purposes in medicine, given their good capacity for cell proliferation and differentiation. Although BMSCs have been widely studied, recent hADSCs have attracted a lot of attention because they can be easily obtained in large quantities with the lowest cost and they have useful properties compared to BMSCs [18].

In this study, PCL/Gel composite fibers with and without nHA and Vitamin D3 were constructed by electrospinning method and the morphology of the scaffolds was investigated.

The collected fibers were composed of single, homogeneous and random morphology, and no visible beads or small and broken fibers were found in any of the scaffolds. Also, nHA was well incorporated into the fibers. In consistent with previous researches at this study, smooth and bead-free morphology with a uniform size of fibers and optimal porosity percent with appropriate size was observed for PCL/Gel/nHA, PCL/Gel/Vit D3 and PCL/Gel/nHA/Vit D3 composite scaffolds [7].

EDX spectral showed the presence of Ca-P in PCL/Gel/Vit D3 scaffold contains 20% HA (Figure 2a). The spectral map scan confirmed that nHA particles were dispersed randomly within PCL/Gel/nHA/Vit D3 scaffold.

The TEM image showed a roughly flat surface of the fibers, which confirms the presence of nHA particles inside the fibers and a uniform distribution of them. But in some parts, the tendency to particle agglomeration is well observed, as this particle accumulation can be due to the high tendency of particles to reduce their surface energy.

The FTIR spectrum of PCL/Gel composite scaffold showed all PCL and Gel characteristic bonds. On the other hand, the appearance of all PCL/Gel and nHA characteristic bonds in PCL/Gel/nHA composite fibers confirms the successful blending of HA in PCL/Gel composite scaffold. Due to the small proportion of the initial amount of vitamin D3 in comparison to other composite scaffold components, the assigned peaks for vitamin D3 were weaker than the other components and overlapped in some situations with PCL characteristic bonds.

The release profiles of vitamin D3 from PCL/Gel/nHA/Vit D3 scaffold have been studied in water/ethanol medium (pH=7.4) for 30 days at 37 °C (Figure 5). In general, gelatin in PCL/Gel/nHA/Vit D3 scaffold acts as a prose-forming agent, and creates channels in the polymer due to its high solubility in aqueous solutions, and provides infiltration routes of water molecules across the polymers, and PCL hydraulic degradation also increases [34]. These channels induced by polymer degradation and solubility accelerate the release of drug molecules from the polymer matrix to the release medium [35]. On the other hand, the addition of hydroxyapatite nanoparticles increases the surface contact of nanoparticles and polymers, and further expands the polymer structure [35] and increases the infiltration of water into the polymer and enhances the release of vitamin D3 molecules into its release medium. PCL/Gel/nHA composite with 2% vitamin D3 gave about 7% release of vitamin D3 within 24 h with a smooth and regulated release thereafter. PCL/Gel/nHA composite with 5% vitamin D3 (Figure 5) releases vitamin D3 much more rapidly than the 2% sample. The initial rate of release of PCL/Gel/nHA composite with 5% vitamin D3 is high during the first day, most likely due to release of drug sequestered on the sample surfaces. Rapid release on the web containing 5% vitamins may be due to the dissolution and penetration of the drug. Since the drug dosage in this scaffold is higher, thus the drug molecules are not completely loaded in the polymer matrix and are accumulated mostly in

proximity and over the fiber surface [36]. Therefore, when the scaffold is in release medium, the drug molecules enter the medium quickly and, as a result, we will see a rapid release of vitamin D3 within the early hours of the web containing 5% vitamin. In lower dose of vitamin D3 (2% vitamin) loading, the web of nanofibers showed a slow, constant and controlled release of the drug, which is related to the drug infiltration into the polymer matrix, and the drug was released stably from the composite scaffold.

In the next stage, cell culture was studied on PCL/Gel scaffold with and without nHA and vitamin D3 to obtain suitable a culture method or scaffold for proliferation of osteoblast cells.

As shown in Figure 7, all of the scaffolds showed better cell viability compared to the control sample (in 4 and 7 days). PCL/Gel/nHA and PCL/Gel/Vit D3 scaffolds improved the cellular survival compared to PCL/Gel, significantly ($P < 0.05$). By adding nHA improved significantly ($P < 0.05$) the cell proliferation of PCL/Gel/nHA scaffold compared to PCL/Gel within 7 days. This result may prove the inductive role of HA nanoparticles in the cell proliferation and adhesion. The positive effect of nHA on increasing the proliferation of pig and rat mesenchymal stem cells is also indicated by other researchers [37]. Similarly, the enhanced cell proliferation on scaffold containing HA fibers was also shown by Jaiswal et al [38]. On the other hand, the cell viability was enhanced by the addition of vitamin D3 on days 4 and 7. This may be the result of vitamin D3 intervention in the cellular growth and proliferation. Similarly, Fayyazbakhsh et al., observed a significant increase in cell proliferation by adding vitamin D3 to Hydroxides-Hydroxyapatite/Gelatin/ vitamin D3 scaffold [39]. The results also showed that the combination of HA nanoparticles and vitamin D3 with PCL/Gel scaffold could significantly increase ($P < 0.05$) the proliferation of hADSCs. According to the obtained results, the scaffolds not only had no toxic effects on the cells but also led to the well growth of the cells.

By comparing the scanning electron microscope images, increased cell proliferation can be observed in all the scaffolds 7 days after culture. However, PCL/Gel/nHA and PCL/Gel/Vit D3 scaffolds revealed greater cell proliferation and adhesion compared to the pure PCL/Gel scaffold. This, on the one hand, can be due to the direct effect of vitamins D3, which led to absorption of more proteins of the culture environment. Furthermore, the cells have been larger on the surface of vitamin D3-containing scaffolds that can be a result of the interference of vitamin D3 on the cellular growth. It is clear that the conformation of cytoskeleton reinforced by vitamin D3 and the cell morphology has been transformed from nearly a rounded shape to a more spread star-like shape. On the other hand, this improvement in cellular growth and cell adhesion on PCL/Gel/nHA scaffold is considered to be a specific biological role for nHA particles. The presence of nHA in PCL/Gel scaffold stimulated the osteogenic properties of the cells. Hoang et al., stated that nHA particles are deeply involved in the initial protein adsorption, particularly in the selective attraction of many adhesion proteins including fibronectin, vitronectin, and bone-specific proteins [40]. Similarly, Jaiswal et al., reported that the presence of nHA particles on the surface of scaffold increase the surface area as well as the surface roughness promote the adhesion and proliferation of cells [38]. Our results were consistent with the results of Tamjid et al., who stated in their study that the addition of nanoparticles to the polymer surface increased the effective level of particle contact with cells due to the higher tendency of nanoparticles to accumulate in the surface [41]. In addition, these nanoparticles have an effect on cell adhesion, proliferation and differentiation by creating nanotopography and increasing roughness and surface stiffness. On the 7th day, SEM images displayed a higher cell density in PCL/Gel/nHA/Vit D3 scaffold. The simultaneous presence of HA nanoparticles and vitamin D3 increased the proliferation and adhesion of cells on PCL/Gel/nHA/Vit D3 scaffold, as compared

to the two other scaffolds. The results showed good biocompatibility as well as proper and normal adhesion, expansion and differentiation of PCL/Gel/nHA/Vit D3 scaffold on both the days 1 and 7 after culture.

ALP activity is one of the main osteoblast phenotype expression markers. The results showed a similar trend at day 14 for ALP activity of scaffolds and all scaffolds increased ALP activity more than the control sample ($P < 0.05$). Also, PCL/Gel/Vit D3 scaffold exhibited a better ALP activity than PCL/Gel/nHA, hence, it can be concluded that vitamin D3 has influenced ALP activity stronger than HA ($P < 0.05$). In this study, PCL/Gel/nHA/Vit D3 scaffold exhibited the best ALP activity among the other scaffolds and control sample, significantly ($P < 0.05$). The high ALP activity observed on PCL/Gel/nHA/Vit D3 scaffold compared to the other scaffolds may be due to the synergistic effect of HA nanoparticles and vitamin D3. HA nanoparticles have a crystalline structure similar to the bone mineral phase and are considered as the "gold standard" of grafting materials and vitamin D3 has a direct effect on increased ALP activity due to increased production of calcium precipitation and hence, an increase in matrix mineralization content. Therefore, it can be said that the ALP activity is enhanced by HA and vitamin D3 due to the direct effect of calcium and phosphate of HA, and indirect effect of vitamin D3 on calcium and phosphate regulation via the cell membrane ion channels. These observations were in agreement with other studies, in which ALP activity increased with adding HA [42]. Similarly, Song et al., studied the effect of vitamin D3 on osteogenic differentiation of ADSCs [17]. They observed that with the addition of vitamin D3, the ALP activity increases in the early stages (on day 7). As a result, vitamin D3 promoted the osteogenic differentiation of ADSCs [17]. The increased ALP activity on the 7th to 14th days can be due to entering into the stage of ECM

development and maturity, which is observable with increasing ALP activity. As shown in Figure 9, ALP activity of the scaffolds on the 21st day was associated with a decrease. Reduction of ALP activity during 14 to 21 days after culture for all the scaffolds can be attributed to the complete maturity of ECM and the qualification and preparation of the scaffolds for entering into the mineralization stage. This pattern has been acceptable by the prior results [43], therefore, it can be said that the scaffolds enhanced the osteoblastic phenotype expression as the specific function of natural bone. There is also a general consensus between the findings of the present study and the findings obtained by Nigiam et al., based on which there is an increased ALP activity in PLGA/HA scaffold [44]. In light of these results, it is observed that hADSCs are well reproduced on this composite scaffold and organized to achieve a PCL/Gel/nHA/Vit D3 mineral matrix in order to be used for bone tissue engineering in vitro.

In the present work, we observed an increase of mineral deposition by Von Kossa and Alizarin red staining on the scaffolds. The staining of mineral deposits 21 days after culture shows that the amount of mineral deposits in PCL/Gel/nHA/Vit D3 scaffold matrix was more than that in PCL/Gel/nHA and PCL/Gel/Vit D3 scaffolds within the same period. Moreover, the semi-quantitative analysis performed by extraction of Alizarin red spots shows that PCL/Gel/Vit D3 scaffold exhibited the mineral deposition more than PCL/Gel/nHA. According to the results, the vitamin D3 containing scaffolds facilitate the calcium mineralization due to the effect of vitamin D3 on calcium regulation. Vitamin D3 has a key role in the bone mineralization due to ionic regulation and ALP activity [45]. As a major result of biological evaluation, it seems that vitamin D3 acted as a signaling factor to enhance the osteoblastic activity and bone regeneration. On the other hand, nHA particles can be a template for secondary HA formation, and therefore a

template for the in vitro biomineralization process. Based on the results PCL/Gel/nHA/Vit D3 scaffold due to the simultaneous presence of HA nanoparticles (with a crystalline structure similar to the bone mineral phase) and vitamin D3 exhibited highest amount of mineral deposits compared to the other scaffolds.

Real-time PCR method was conducted to determine the expression of osteogenic markers such as COLL I, ALP, RUNX2 and BGLAP of differentiated cells on the scaffolds. According to the our results, PCL/Gel/nHA and PCL/Gel/Vit D3 scaffolds provided a suitable medium for maintaining the differentiation of osteoblasts; however, PCL/Gel/Vit D3 scaffold showed a higher expression level of bone genes as compared to PCL/Gel/nHA. On the other hand, PCL/Gel/nHA scaffold containing vitamin D3 has revealed far higher expression levels for specific osteoblast genes. Earlier in the study of Kato et al., it was shown that vitamin D3 could be a potent accelerator of osteodifferentiation, particularly from late- to early-phase osteocytes. They showed that treatment with vitamin D3 increased all osteoblast markers in iPSop-day4 cells and MSCop-day4 cells [13]. As previously mentioned, it seems that vitamin D3 acted as a signaling factor to enhance the osteoblastic activity and bone regeneration. On the other hand, Chen et al., found that HA nanoparticles have a significant effect on osteogenic differentiation of mesenchymal stem cells since it stimulates the expression of bone genes [46]. Another study also reported that HA with a specific molecular weight and dose increases osteogenic and osteoconductivity properties [47]. Therefore, it can be argued that the presence of nHA and vitamin D3 in a scaffold leads to a much better growth and differentiation of osteoblasts and better bone tissue production since they simulate a medium like an extracellular matrix for cells. The present study indicates that vitamin D3 and HA affect the process of osteogenic differentiation of mesenchymal stem cells. From the

comparison of osteogenic related genes among groups can be found that COLL I and BGLAP exhibited higher levels of expression and ALP and RUNX2 lower expression levels in all groups. On the other hand, mRNA level of COLL I, BGLAP, ALP and RUNX2 in all scaffolds significantly increased when culture was carried out in the bone induction medium, as compared to the cell culture medium. Based on these results, it was shown that the scaffolds and bone induction medium have a more suitable environment for the differentiation of adipose tissue stem cells than the cell culture medium. Therefore, it can be concluded that many parameters can direct the stem cells derived from adipose tissue towards the bone. For example, the proper scaffold and the use of a bone differentiation medium are factors playing an important role in bone formation and have a great impact on cellular differentiation. The findings of the present study were consistent with Kulterer [48]. They showed that the bone formation at laboratory conditions is carried out in 3 stages:

1. ECM bio-proliferation and synthesis
2. ECM development and maturation through increasing ALP activity
3. ECM mineralization where HA is organized and deposited.

In the first stage after cell culture, the cells are actively proliferated (for the first 10 to 12 days after culture) and several genes associated with the formation of ECM, including COLL I, are seriously expressed. Subsequently, the proliferation rate gradually decreases and ECM maturity begins. Immediately after this decrement in proliferation, ALP activity is greatly increased. This occurs during the days 12 and 18. At this time, ECM is matured and qualified to be mineralized. In the third stage of bone growth, ALP expression is reduced and other genes associated with bone mineralization, such as BGLAP, are expressed at the maximum level.

According to the findings of this study and Kulterer et al., it can be concluded that increasing the expression of BGLAP gene on day 21 may be related to the final stage of bone formation, i.e. ECM mineralization along with the calcium precipitation [48].

On the other hand, the reduced expression of ALP gene during the same period can be attributed to the complete maturity of ECM and the qualification and preparation of scaffolds for entering the mineralization stage. COLL I, known as an early marker of osteoprogenitor cells, increased throughout this period. RUNX2 gene is expressed during the bone formation period; however, the differentiation is accompanied with different expressions at different times. The information driven from real time-PCR profile revealed the expected expression of the bone phenotype.

5. CONCLUSIONS

In this study, the electrospun nanocomposite scaffold with novel combination of PCL/Gel/nHA/Vit D3 was presented to use in bone tissue engineering. A smooth and bead-free morphology with uniform fiber diameter size and optimal porosity with appropriate size was observed for all scaffolds. In FTIR spectrum of PCL/Gel/nHA/Vit D3 composite fiber, appeared all the characteristic peaks of PCL/Gel/nHA and Vit D3, which confirmed the successful integration of nHA and Vit D3 into PCL/Gel composite scaffolds. Release of vitamin D3 from electrospun fibers of PCL/Gel/nHA/Vit D3 composite was studied and it was found that electrospun PCL/Gel/nHA containing 2% vitamin D3 fiber gave relatively smooth release of drug over about 30 days. In addition, the culture hADSCs on novel combination of PCL/Gel/nHA/Vitamin D3 was performed and analyzed. The results of cell toxicity and proliferation showed that electrospun composite scaffolds were biocompatible and had no negative effect on adipose tissue stem cells in vitro. The results of hADSCs cultured on the

scaffolds revealed the normal morphology and proper adhesion of all scaffolds. The simultaneous effect of the use of HA nanoparticles and vitamin D3 on osteogenic differentiation of hADSCs and calcification of scaffolds was studied. As the main indicators of osteoconductivity, the calcium deposition and ALP activity have promoted significantly because of the direct effect of HA and indirect intervention of vitamin D3 in the calcium and phosphate regulation. In particular, the cells cultured on PCL/Gel/nHA/Vit D3 scaffold had a significant increase in terms of ALP activity (on the 14^{th} day) and scaffold mineralization (on the 21^{st} day) compared to the two other scaffolds, indicating that vitamin D3 and HA increase the osteogenic differentiation of hADSCs. It was found that the treatment with nHA and vitamin D3 for 21 days not only increases mineralization but also upregulates the expression of osteoblast markers, including ALP, COLL I, BGLAP and RUNX2, in hADSCs cells. Additionally, when the adipose tissue stem cells were induced with osteogenic medium, the expression of specific bone genes significantly increased. These findings suggest that hADSCs can be used for osteogenic differentiation to reduce the cost imposed by a clinical program. Using HA nanoparticles and vitamin D3, a method could be developed to induce beneficial and cost-effective bone formation caused by hADSCs in bone tissue engineering.

ACKNOWLEDGMENTS

The authors gratefully acknowledge Iranian National Science Foundation (INSF) for their financial (grant No: 95813894) support and Central Research Laboratories of Isfahan University of Medical Sciences for using their facilities during histological preparation of samples.

REFERENCES

1. Li, Z., & Li, Z. B. (2005). Repair of mandible defect with tissue engineering bone in rabbits. ANZ journal of surgery, 75(11), 1017-1021.
2. Cassidy, J. W. (2014). Nanotechnology in the regeneration of complex tissues. Bone and tissue regeneration insights, 5, 25.
3. Khorshidi, S., Solouk, A., Mirzadeh, H., Mazinani, S., Lagaron, J. M., Sharifi, S., & Ramakrishna, S. (2016). A review of key challenges of electrospun scaffolds for tissue-engineering applications. Journal of tissue engineering and regenerative medicine, 10(9), 715-738.
4. Vatankhah, E., Semnani, D., Prabhakaran, M. P., Tadayon, M., Razavi, S., & Ramakrishna, S. (2014). Artificial neural network for modeling the elastic modulus of electrospun polycaprolactone/gelatin scaffolds. Acta biomaterialia, 10(2), 709-721.
5. Yoshimoto, H., Shin, Y. M., Terai, H., & Vacanti, J. P. (2003). A biodegradable nanofiber scaffold by electrospinning and its potential for bone tissue engineering. Biomaterials, 24(12), 2077-2082.
6. Gautam, S., Chou, C. F., Dinda, A. K., Potdar, P. D., & Mishra, N. C. (2014). Fabrication and characterization of PCL/gelatin/chitosan ternary nanofibrous composite scaffold for tissue engineering applications. *Journal of materials science*, *49*(3), 1076-1089.
7. Denis, P., Dulnik, J., & Sajkiewicz, P. (2015). Electrospinning and structure of bicomponent polycaprolactone/gelatin nanofibers obtained using alternative solvent system. International Journal of Polymeric Materials and Polymeric Biomaterials, 64(7), 354-364.

8. Hench, L. L.; Polak, J. M., “Third-Generation Biomedical Materials”, 8 VOL 295 SCIENCE, FEBRUARY (2002).
9. Wutti charoenmongkol, P., Sanchavanakit, N., Pavasant, P., & Supaphol, P. (2006). Preparation and characterization of novel bone scaffolds based on electrospun polycaprolactone fibers filled with nanoparticles. Macromolecular bioscience, 6(1), 70-77.
10. Yu, H. S., Jang, J. H., Kim, T. I., Lee, H. H., & Kim, H. W. (2009). Apatite-mineralized polycaprolactone nanofibrous web as a bone tissue regeneration substrate. Journal of Biomedical Materials Research Part A, 88(3), 747-754.
11. Venkatesan, J., & Kim, S. K. (2014). Nano-hydroxyapatite composite biomaterials for bone tissue engineering—a review. Journal of biomedical nanotechnology, 10(10), 3124-3140.
12. Ghomi, H., Fathi, M. H., & Edris, H. (2011). Preparation of nanostructure hydroxyapatite scaffold for tissue engineering applications. Journal of sol-gel science and technology, 58(3), 642-650.
13. Kato, H., Ochiai-Shino, H., Onodera, S., Saito, A., Shibahara, T., & Azuma, T. (2015). Promoting effect of 1, 25 (OH) 2 vitamin D3 in osteogenic differentiation from induced pluripotent stem cells to osteocyte-like cells. Open biology, 5(2), 140-201.
14. Lien, Y. H., Wu, J. H., Liao, J. W., & Wu, T. M. (2013). In vitro evaluation of the thermosensitive and magnetic nanoparticles for the controlled drug delivery of vitamin D3. Macromolecular Research, 21(5), 511-518.
15. Mason, S. S., Kohles, S. S., Winn, S. R., & Zelick, R. D. (2013). Extrahepatic 25-Hydroxylation of Vitamin D3 in an Engineered Osteoblast Precursor Cell Line Exploring

the Influence on Cellular Proliferation and Matrix Maturation during Bone Development. ISRN Biomedical Engineering, 2013.

16. Curtis, K. M., Aenlle, K. K., Roos, B. A., & Howard, G. A. (2014). 24 R, 25-Dihydroxyvitamin D3 Promotes the Osteoblastic Differentiation of Human Mesenchymal Stem Cells. Molecular endocrinology, 28(5), 644-658.
17. Song, I., Kim, B. S., Kim, C. S., & Im, G. I. (2011). Effects of BMP-2 and vitamin D 3 on the osteogenic differentiation of adipose stem cells. Biochemical and biophysical research communications, 408(1), 126-131.
18. Fink, T., Lund, P., Pilgaard, L., Rasmussen, J. G., Duroux, M., & Zachar, V. (2008). Instability of standard PCR reference genes in adipose-derived stem cells during propagation, differentiation and hypoxic exposure. BMC molecular biology, 9(1), 98.
19. Liu, H., Ding, X., Zhou, G., Li, P., Wei, X., & Fan, Y. (2013). Electrospinning of nanofibers for tissue engineering applications. Journal of Nanomaterials, 2013, 3.
20. Nguyen, T. U., Tey, S. Y., Pourgholami, M. H., Morris, D. L., Davis, T. P., Barner Kowollik, C., & Stenzel, M. H. (2007). Synthesis of semi-biodegradable crosslinked microspheres for the delivery of 1, 25 dihydroxyvitamin D3 for the treatment of hepatocellular carcinoma. European polymer journal, 43(5), 1754-1767.
21. Shokrgozar, M. A., Fattahi, M., Bonakdar, S., Kashani, I. R., Majidi, M., Haghighipour, N & Saeedi, S. N. (2012). Healing potential of mesenchymal stem cells cultured on a collagen-based scaffold for skin regeneration. Iranian biomedical journal, 16(2), 68.
22. Naeimi, M., Rafienia, M., Fathi, M., Janmaleki, M., Bonakdar, S., & Ebrahimian-Hosseinabadi, M. (2016). Incorporation of chitosan nanoparticles into silk fibroin-based

porous scaffolds: Chondrogenic differentiation of stem cells. International Journal of Polymeric Materials and Polymeric Biomaterials, 65(4), 202-209.

23. Marino, G., Rosso, F., Cafiero, G., Tortora, C., Moraci, M., Barbarisi, M., & Barbarisi, A. (2010). β-Tricalcium phosphate 3D scaffold promote alone osteogenic differentiation of human adipose stem cells: in vitro study. Journal of Materials Science: Materials in Medicine, 21(1), 353-363.
24. Mehrasa, M., Anarkoli, A. O., Rafienia, M., Ghasemi, N., Davary, N., Bonakdar, S., ... & Salamat, M. R. (2016). Incorporation of zeolite and silica nanoparticles into electrospun PVA/collagen nanofibrous scaffolds: The influence on the physical, chemical properties and cell behavior. International Journal of Polymeric Materials and Polymeric Biomaterials, 65(9), 457-465.
25. Bhardwaj, N., & Kundu, S. C. (2010). Electrospinning: a fascinating fiber fabrication technique. Biotechnology advances, 28(3), 325-347.
26. Tirkkonen, L., Halonen, H., Hyttinen, J., Kuokkanen, H., Sievänen, H., Koivisto, A. M., ... & Haimi, S. (2011). The effects of vibration loading on adipose stem cell number, viability and differentiation towards bone-forming cells. Journal of The Royal Society Interface, 8(65), 1736-1747.
27. Tetteh, G., Khan, A. S., Delaine-Smith, R. M., Reilly, G. C., & Rehman, I. U. (2014). Electrospun polyurethane/hydroxyapatite bioactive Scaffolds for bone tissue engineering: The role of solvent and hydroxyapatite particles. journal of the mechanical behavior of biomedical materials, 39, 95-110.
28. Komori, T. (2010). Regulation of bone development and extracellular matrix protein genes by RUNX2. Cell and tissue research, 339(1), 189.

29. Lee, H., Yeo, M., Ahn, S., Kang, D. O., Jang, C. H., Lee, H., ... & Kim, G. H. (2011). Designed hybrid scaffolds consisting of polycaprolactone microstrands and electrospun collagen-nanofibers for bone tissue regeneration. Journal of biomedical materials research Part B: Applied biomaterials, 97(2), 263-270.
30. Causa, F., Netti, P. A., Ambrosio, L., Ciapetti, G., Baldini, N., Pagani, S., ... & Giunti, A. (2006). Poly-□-caprolactone/hydroxyapatite composites for bone regeneration: In vitro characterization and human osteoblast response. Journal of Biomedical Materials Research Part A: An Official Journal of The Society for Biomaterials, The Japanese Society for Biomaterials, and The Australian Society for Biomaterials and the Korean Society for Biomaterials, 76(1), 151-162.
31. Toyran, N., & Severcan, F. (2007). Interaction between vitamin D2 and magnesium in liposomes: Differential scanning calorimetry and FTIR spectroscopy studies. Journal of Molecular Structure, 839(1-3), 19-27.
32. Urankar, M., Reddy, N., & Ranka, V. Formulation Development and Evaluation of Cholecalciferol (Vitamin D3) Granules and Tablets.
33. Amirpour, N., Razavi, S., Esfandiari, E., Hashemibeni, B., Kazemi, M., & Salehi, H. (2017). Hanging drop culture enhances differentiation of human adipose-derived stem cells into anterior neuroectodermal cells using small molecules. International Journal of Developmental Neuroscience, 59, 21-30.
34. Verreck, G., Chun, I., Rosenblatt, J., Peeters, J., Van Dijck, A., Mensch, J., & Brewster, M. E. (2003). Incorporation of drugs in an amorphous state into electrospun nanofibers

composed of a water-insoluble, nonbiodegradable polymer. Journal of Controlled Release, 92(3), 349-360.

35. Kim, H. W., Knowles, J. C., & Kim, H. E. (2004). Effect of biphasic calcium phosphates on drug release and biological and mechanical properties of poly (□-caprolactone) composite membranes. Journal of Biomedical Materials Research Part A, 70(3), 467-479.
36. Kenawy, E. R., Bowlin, G. L., Mansfield, K., Layman, J., Simpson, D. G., Sanders, E. H., & Wnek, G. E. (2002). Release of tetracycline hydrochloride from electrospun poly (ethylene-co-vinylacetate), poly (lactic acid), and a blend. Journal of controlled release, 81(1-2), 57-64.
37. Zou, L., Zou, X., Chen, L., Li, H., Mygind, T., Kassem, M., & Bünger, C. (2008). Effect of hyaluronan on osteogenic differentiation of porcine bone marrow stromal cells in vitro. Journal of Orthopaedic Research, 26(5), 713-720.
38. Jaiswal, A. K., Chhabra, H., Soni, V. P., & Bellare, J. R. (2013). Enhanced mechanical strength and biocompatibility of electrospun polycaprolactone-gelatin scaffold with surface deposited nano-hydroxyapatite. Materials Science and Engineering: C, 33(4), 2376-2385.
39. Fayyazbakhsh, F., Solati-Hashjin, M., Keshtkar, A., Shokrgozar, M. A., Dehghan, M. M., & Larijani, B. (2017). Release behavior and signaling effect of vitamin D3 in layered double hydroxides-hydroxyapatite/gelatin bone tissue engineering scaffold: An in vitro evaluation. Colloids and Surfaces B: Biointerfaces, 158, 697-708.
40. Hoang, Q. Q., Sicheri, F., Howard, A. J., & Yang, D. S. (2003). Bone recognition mechanism of porcine osteocalcin from crystal structure. Nature, 425(6961), 977.

41. Tamjid, E., & Simchi, A. (2015). Fabrication of a highly ordered hierarchically designed porous nanocomposite via indirect 3D printing: Mechanical properties and in vitro cell responses. Materials & Design, 88, 924-931.
42. Dvorak, M. M., & Riccardi, D. (2004). Ca2+ as an extracellular signal in bone. Cell calcium, 35(3), 249-255.
43. Ngiam, M., Liao, S., Patil, A. J., Cheng, Z., Chan, C. K., & Ramakrishna, S. (2009). The fabrication of nano-hydroxyapatite on PLGA and PLGA/collagen nanofibrous composite scaffolds and their effects in osteoblastic behavior for bone tissue engineering. Bone, 45(1), 4-16.
44. Choi, S. W., Zhang, Y., Thomopoulos, S., & Xia, Y. (2010). In vitro mineralization by preosteoblasts in poly (DL-lactide-co-glycolide) inverse opal scaffolds reinforced with hydroxyapatite nanoparticles. Langmuir, 26(14), 12126-12131.
45. Lieben, L., & Carmeliet, G. (2013). Vitamin D signaling in osteocytes: effects on bone and mineral homeostasis. Bone, 54(2), 237-243.
46. Chen, J. P., & Chang, Y. S. (2011). Preparation and characterization of composite nanofibers of polycaprolactone and nanohydroxyapatite for osteogenic differentiation of mesenchymal stem cells. Colloids and Surfaces B: Biointerfaces, 86(1), 169-175.
47. Takahashi, Y., Yamamoto, M., & Tabata, Y. (2005). Osteogenic differentiation of mesenchymal stem cells in biodegradable sponges composed of gelatin and β-tricalcium phosphate. Biomaterials, 26(17), 3587-3596.
48. Kulterer, B., Friedl, G., Jandrositz, A., Sanchez-Cabo, F., Prokesch, A., Paar, C., ... & Trajanoski, Z. (2007). Gene expression profiling of human mesenchymal stem cells

derived from bone marrow during expansion and osteoblast differentiation. BMC genomics, 8(1), 70.

Figures captions

Figure 1: SEM images of fibers at 2500X magnification

Figure 2: (a) The EDX spectrum of PCL/Gel/nHA/Vit D3 composite and (b) EDX element mapping analysis of PCL/Gel/nHA/Vit D3 composite scaffold, (scale bar = 500 μm)

Figure 3: TEM image of PCL/Gel/nHA/Vit D3 fiber

Figure 4: FTIR spectra of PCL, Gel, PCL/Gel, nHA, PCL/Gel/nHA and PCL/Gel/nHA/Vit D3 samples

Figure 5: Cumulative vitamin D3 release profiles from PCL/Gel/nHA with 2 and 5% Vit D3

Figure 6: The image provided by an invert microscope from stem cells cultured on the polystyrene culture flask floor at 40X magnification

Figure 7: Cell proliferation as indicated by MTT assay of hADSCs seeded on scaffolds in bone induction medium (+) after 1, 4 and 7 days, (*): $P< 0.05$

Figure 8: Morphology of hADSCs on scaffolds in bone induction medium (+) after 1 and 7 days of cell seeding at 125X and 500X magnification

Figure 9: ALP analysis on scaffolds in bone induction medium (+) after 7, 14 and 21 days, (*): $P< 0.05$

Figure 10: Von Kossa staining of differentiated hADSCs on scaffolds in bone induction medium (+) after 7 and 21 days of cell seeding at 40X magnification

Figure 11: Alizarin red staining of differentiated hADSCs on scaffolds in bone induction medium (+) after 7, 14 and 21 days at 40X magnification

Figure 12: Quantitative measurements of mineral deposition in differentiated hADSCs by Alizarin red staining on scaffolds in bone induction medium (+) after 7, 14 and 21 days, (*): P< 0.05

Figure 13: Comparison of the results of the gene expression analysis of hADSCs cultured on the scaffolds in both the bone induction and cell culture medium after 21 days, (*): P< 0.05

Figure 14: Comparison of the results of COLL I, BGLAP, ALP and RUNX2 among groups in both the bone induction and cell culture medium after 21 days, (*): P< 0.05

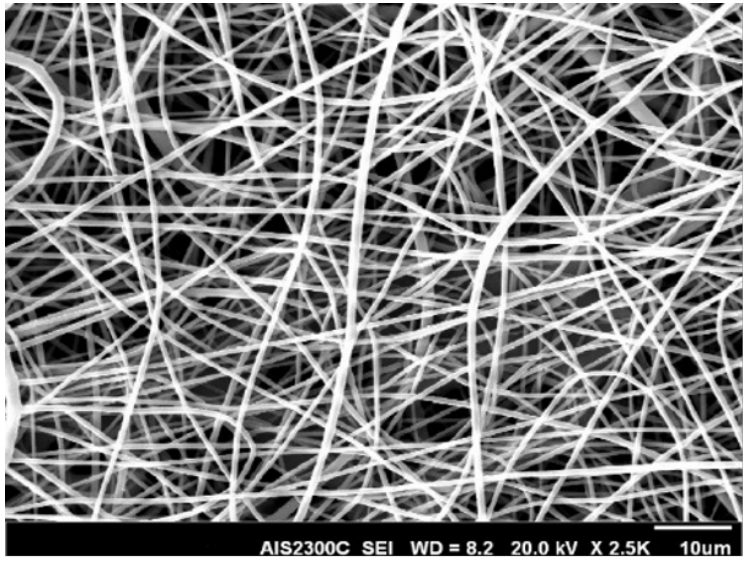

PCL/Gel

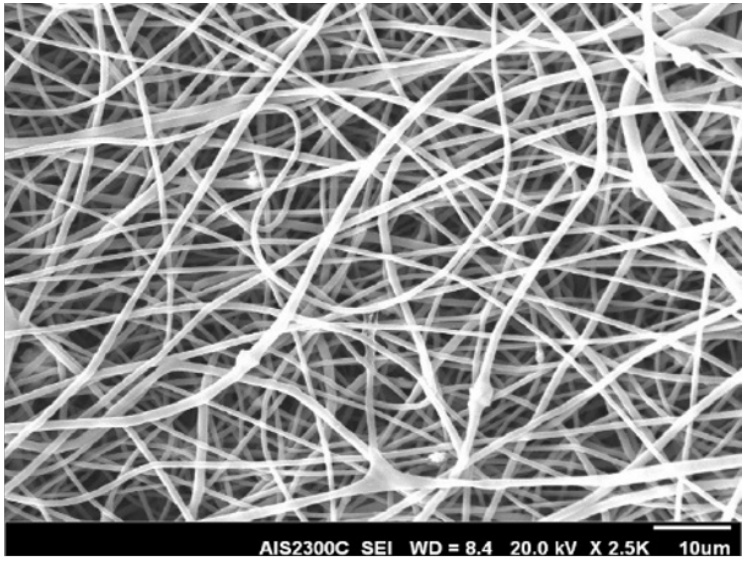

PCL/Gel/nHA

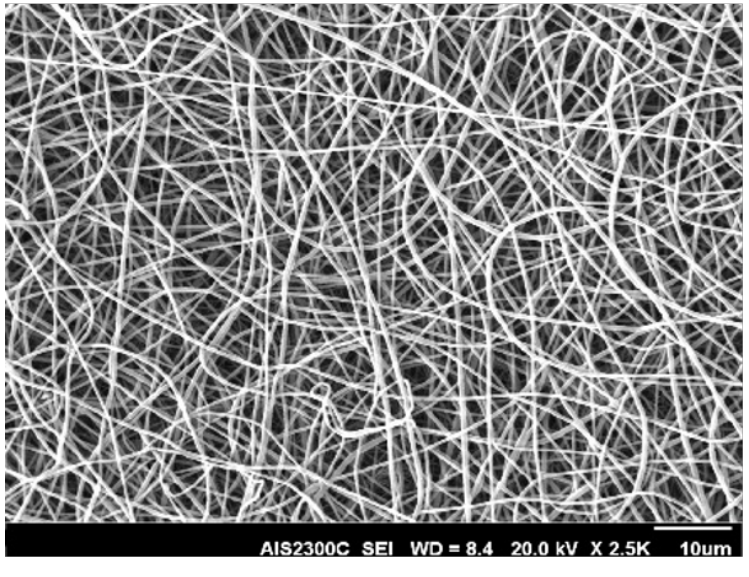

PCL/Gel/Vit D3

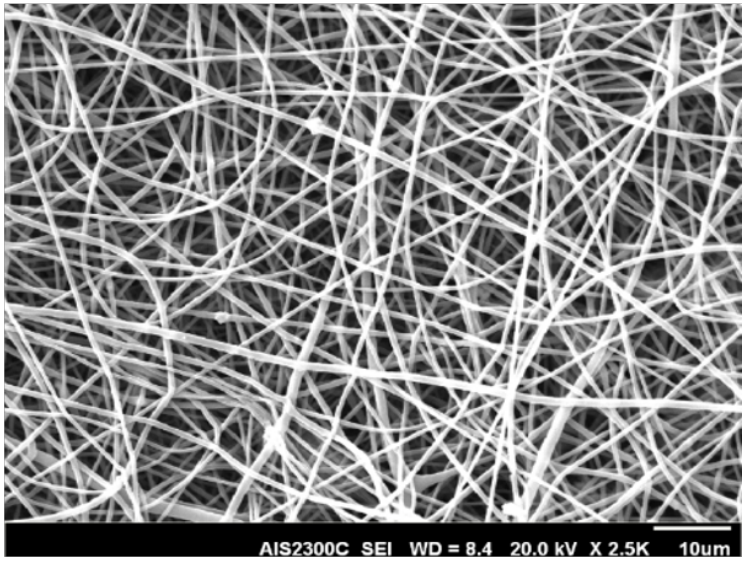

PCL/Gel/nHA/Vit D3

(a)

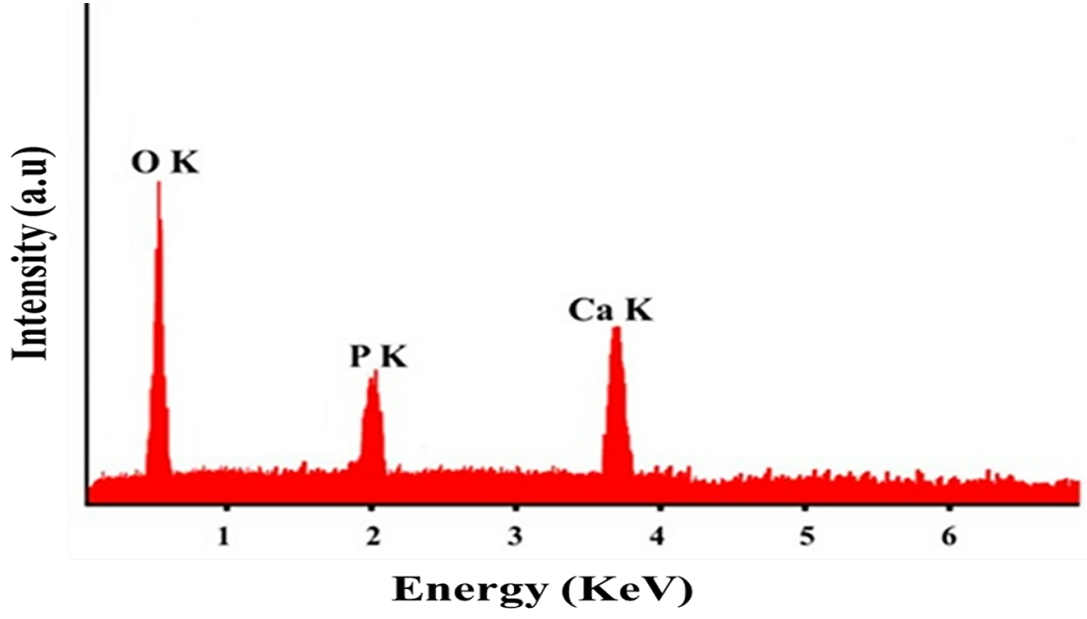
Intensity (a.u)
O K
P K
Ca K
1
2
3
4
5
6
Energy (KeV)

(b)

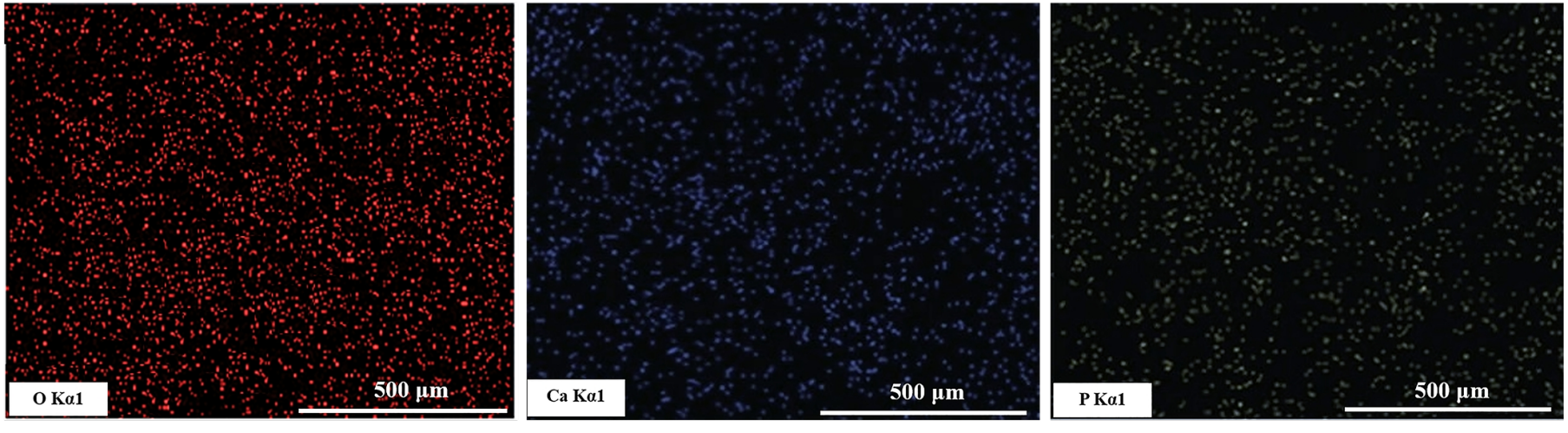
O Kα1
500 µm
Ca Kα1
500 µm
P Kα1
500 µm

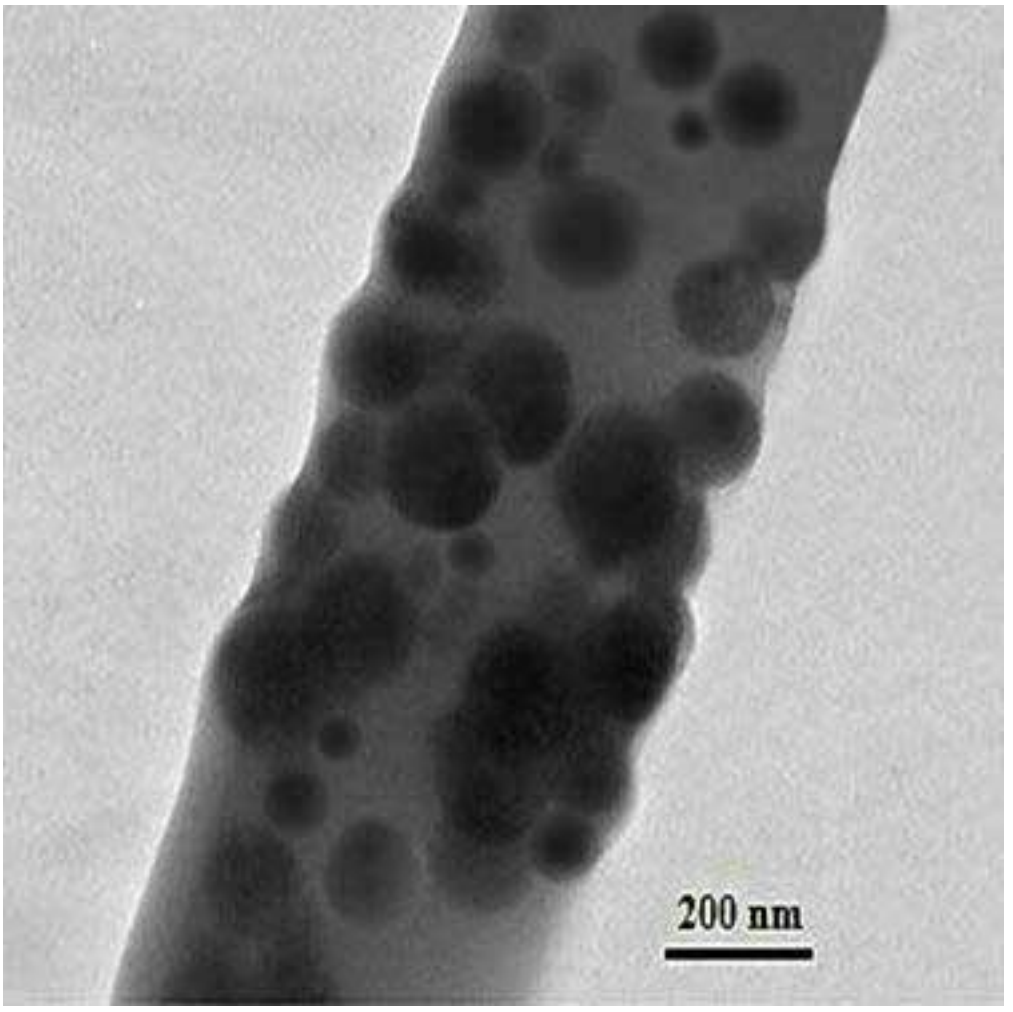
200 nm

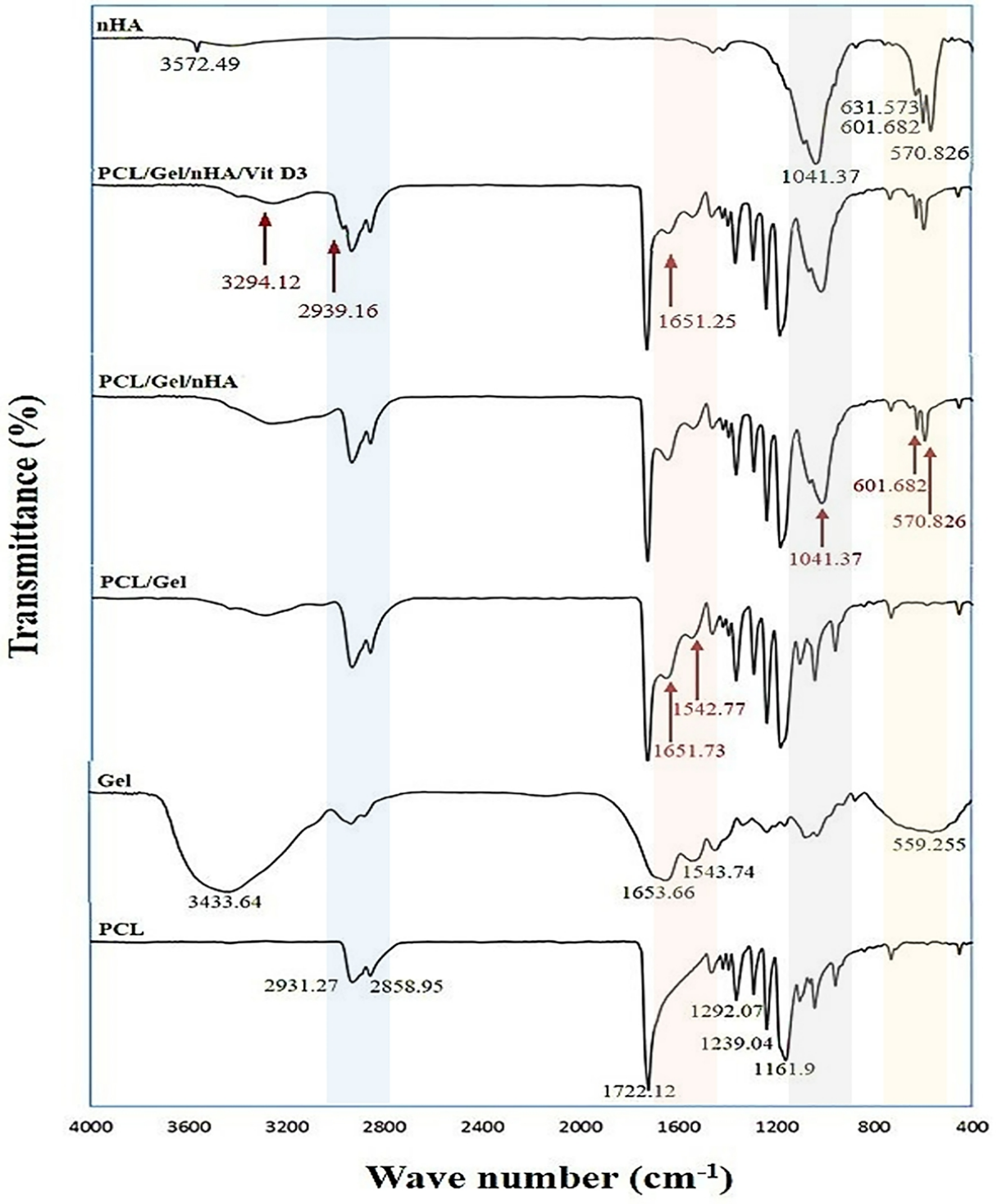
nHA
3572.49
631.573
601.682
570.826
1041.37
PCL/Gel/nHA/Vit D3
3294.12
2939.16
1651.25
PCL/Gel/nHA
601.682
570.826
1041.37
PCL/Gel
1542.77
1651.73
Gel
559.255
1543.74
1653.66
3433.64
PCL
2931.27
2858.95
1292.07
1239.04
1161.9
1722.12
Transmittance (%)
4000
3600
3200
2800
2400
2000
1600
1200
800
400
Wave number (cm-1)

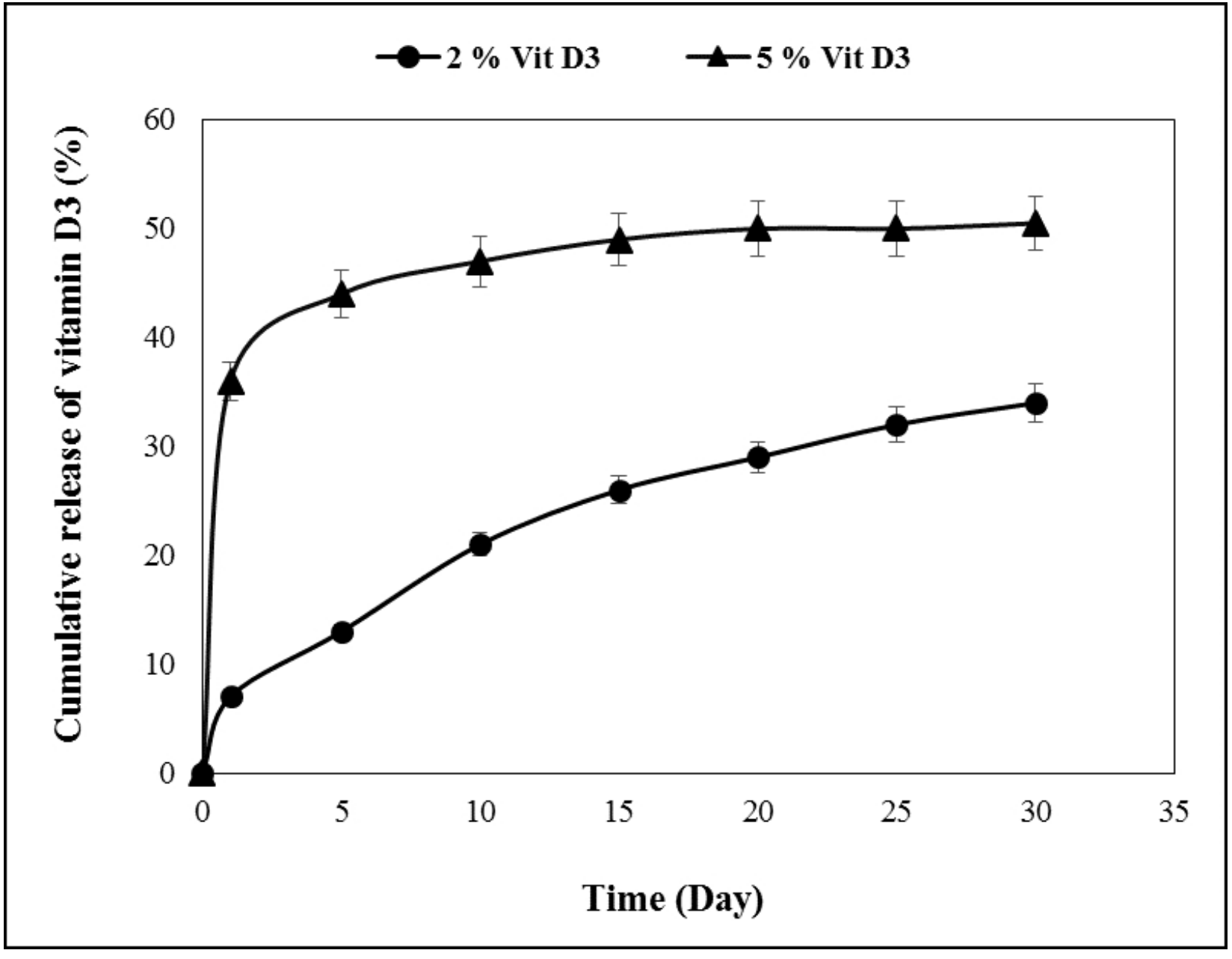
2 % Vit D3
5 % Vit D3
Cumulative release of vitamin D3 (%)
60
50
40
30
20
10
0
0
5
10
15
20
25
30
35
Time (Day)

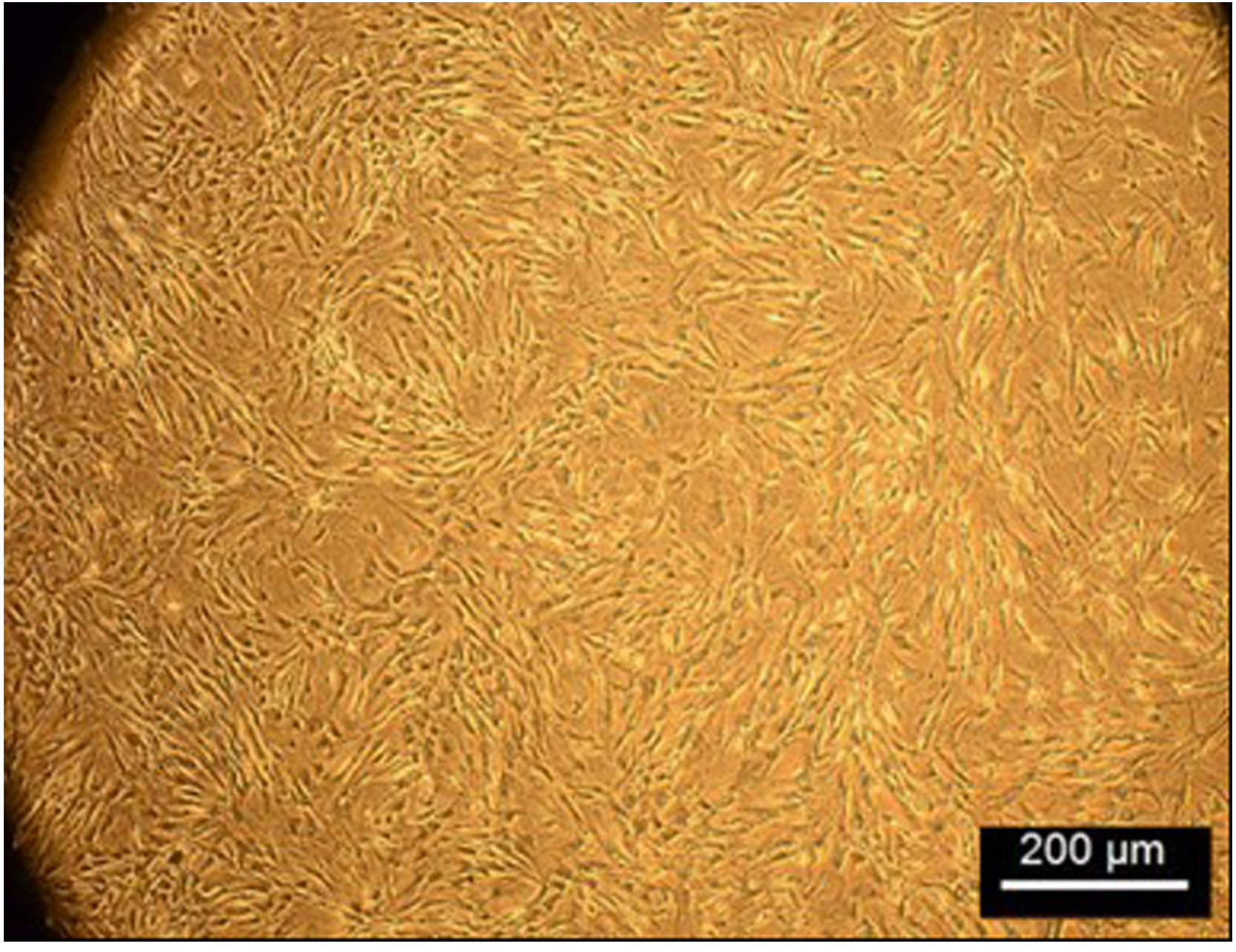
200 µm

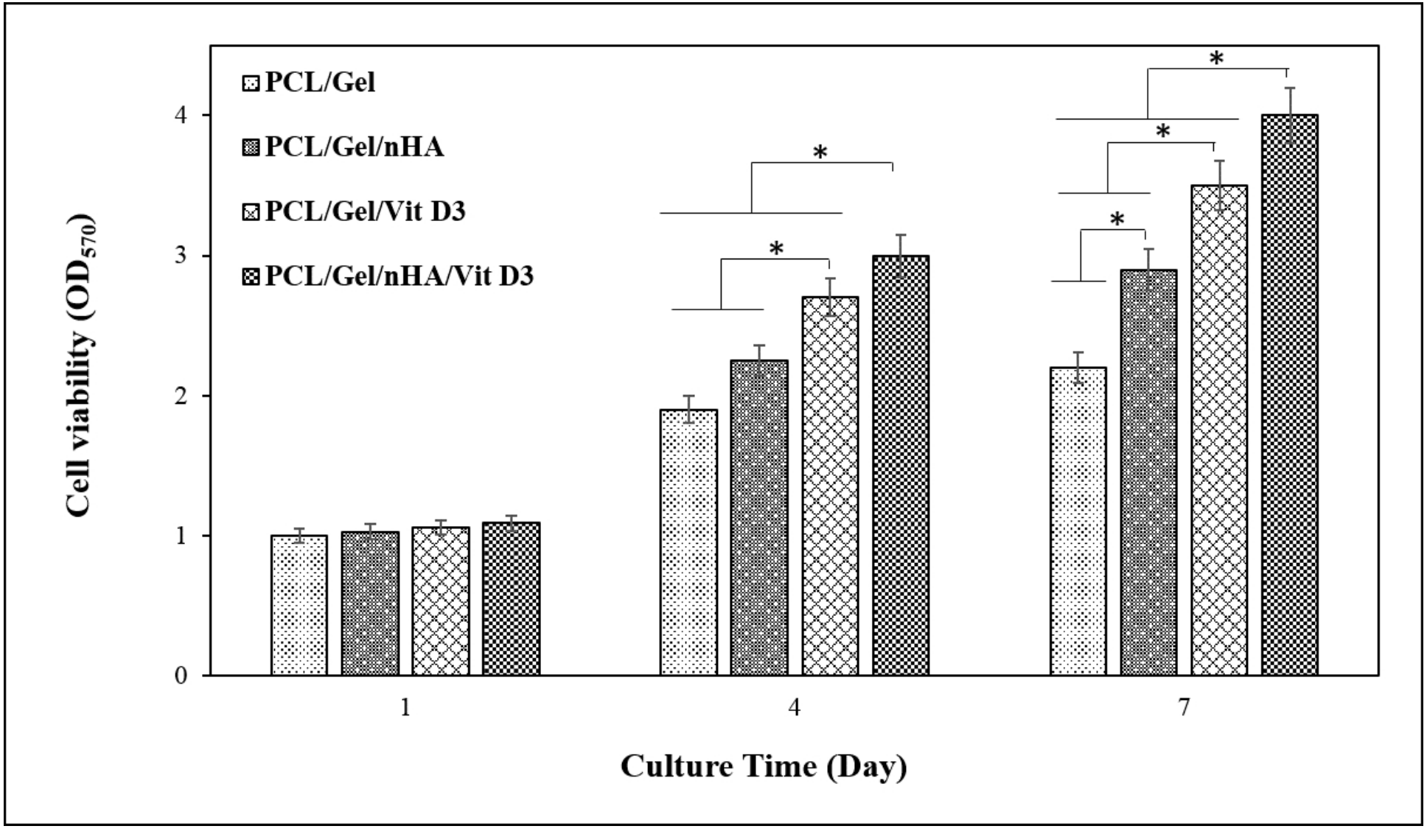
PCL/Gel
PCL/Gel/nHA
PCL/Gel/Vit D3
PCL/Gel/nHA/Vit D3
Cell viability (OD570)
0
1
2
3
4
1
4
7
Culture Time (Day)
*
*
*
*
*

D1
D7
PCL/Gel
PCL/Gel/nHA
PCL/Gel/Vit D3
PCL/Gel/nHA/Vit D3
Spot Magn Det WD
200 µm
4.8 125x SE 9.7
4.8 125x SE 9.1
4.4 125x SE 9.0
5.0 125x SE 9.7
4.6 125x SE 9.6
4.7 125x SE 9.7
4.3 125x SE 9.7

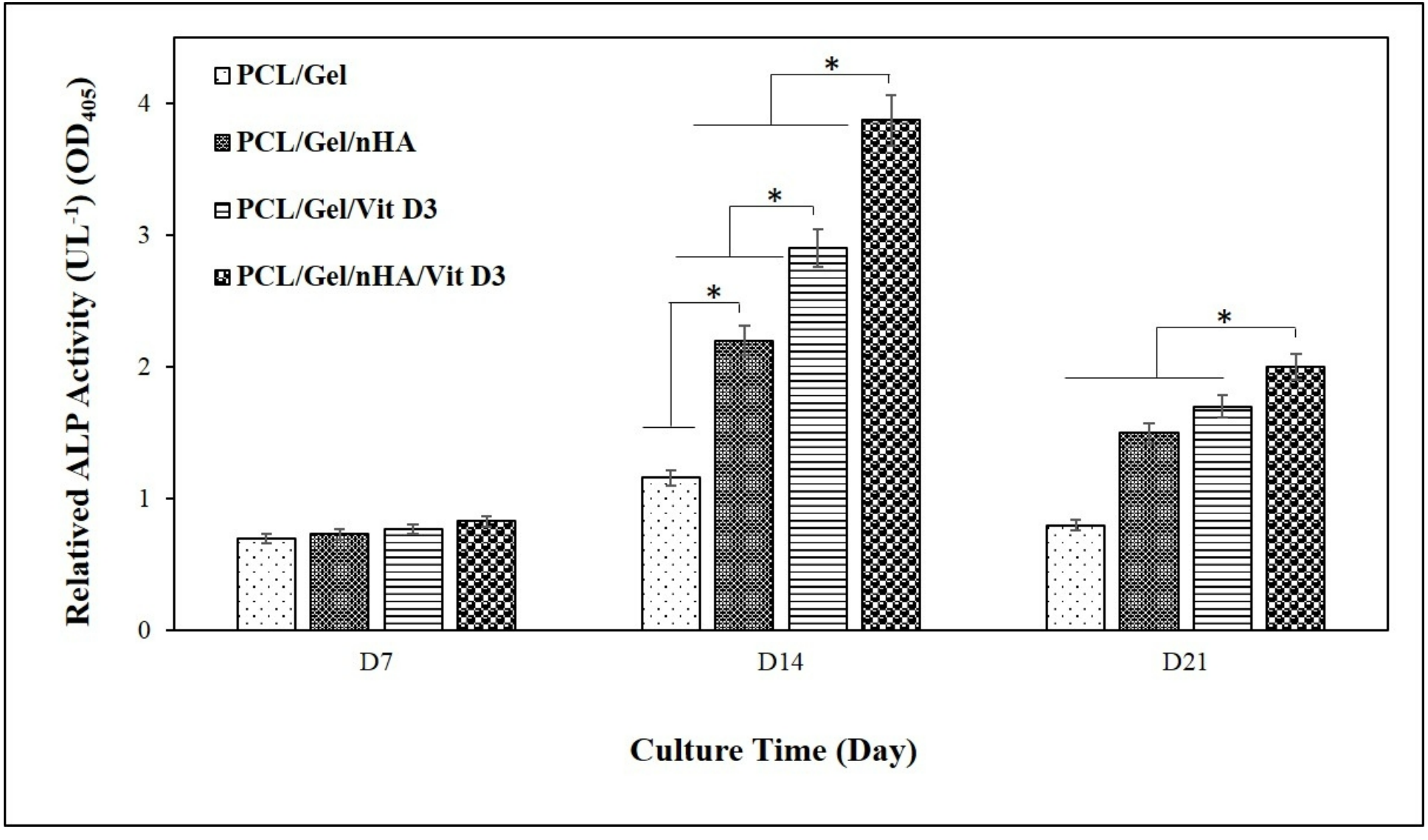
PCL/Gel
PCL/Gel/nHA
PCL/Gel/Vit D3
PCL/Gel/nHA/Vit D3
Relatived ALP Activity (UL-1) (OD405)
0
1
2
3
4
*
*
*
*
D7
D14
D21
Culture Time (Day)

D1
D7
PCL/Gel
PCL/Gel/nHA
PCL/Gel/Vit D3
PCL/Gel/nHA/Vit D3
200 µm

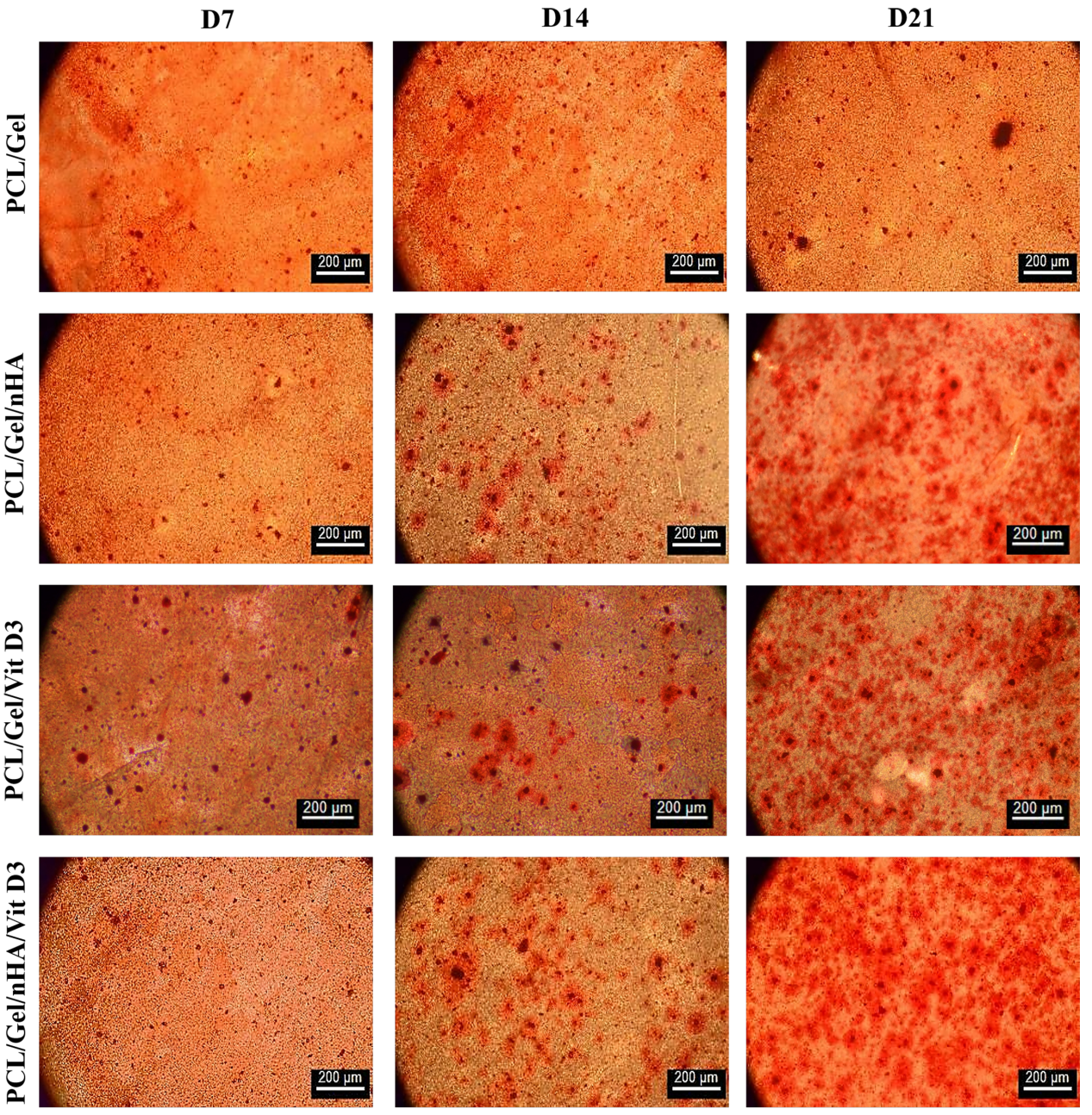
D7
D14
D21
PCL/Gel
PCL/Gel/nHA
PCL/Gel/Vit D3
PCL/Gel/nHA/Vit D3
200 µm

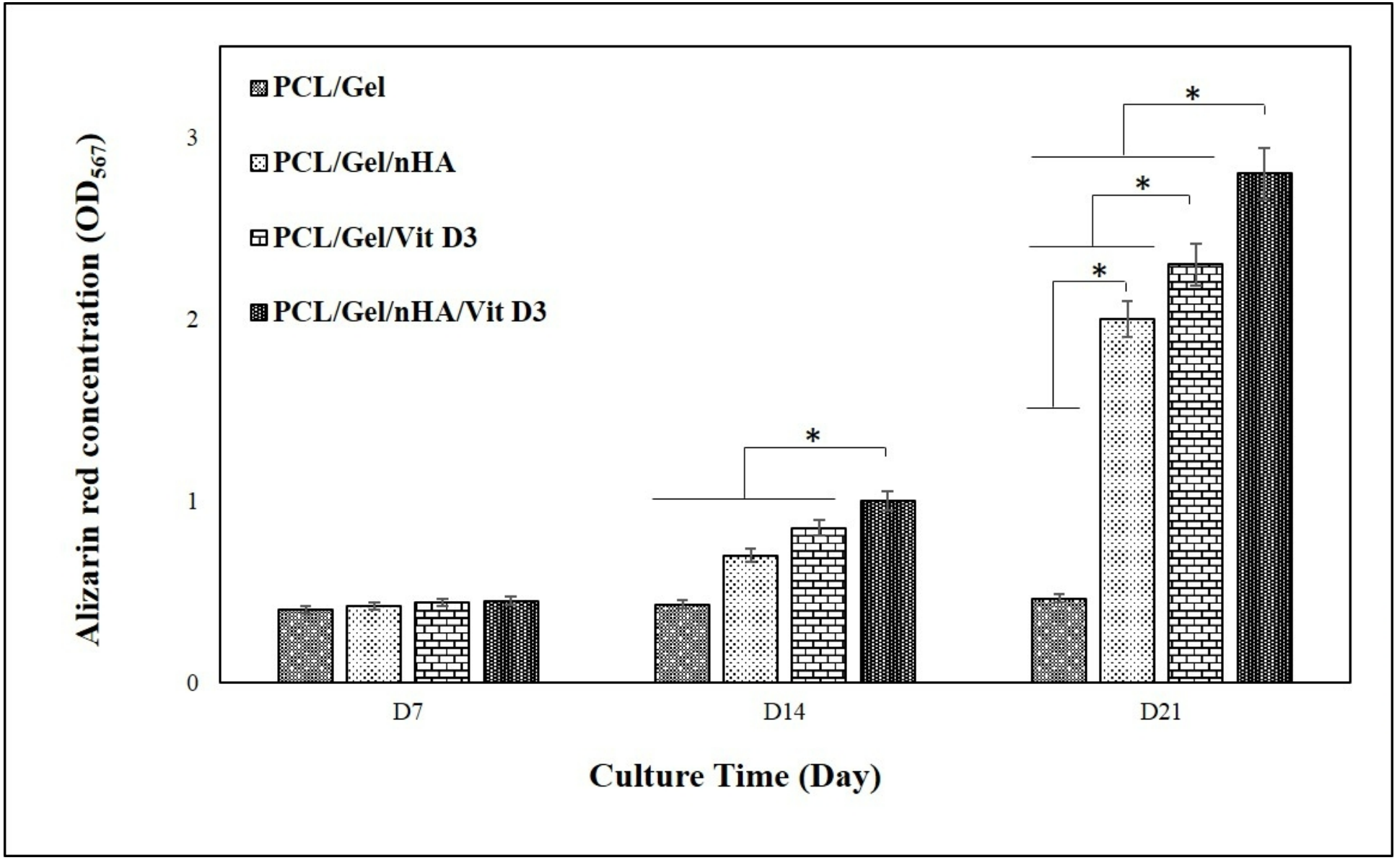
PCL/Gel
PCL/Gel/nHA
PCL/Gel/Vit D3
PCL/Gel/nHA/Vit D3
Alizarin red concentration (OD567)
0
1
2
3
D7
D14
D21
Culture Time (Day)
*
*
*
*

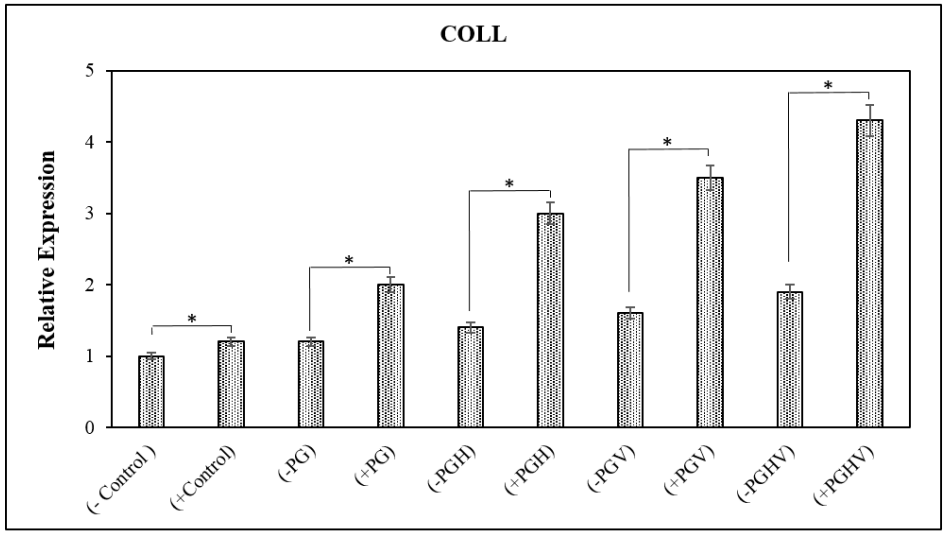
COLL
Relative Expression
0
1
2
3
4
5
*
(- Control)
(+Control)
(-PG)
(+PG)
(-PGH)
(+PGH)
(-PGV)
(+PGV)
(-PGHV)
(+PGHV)

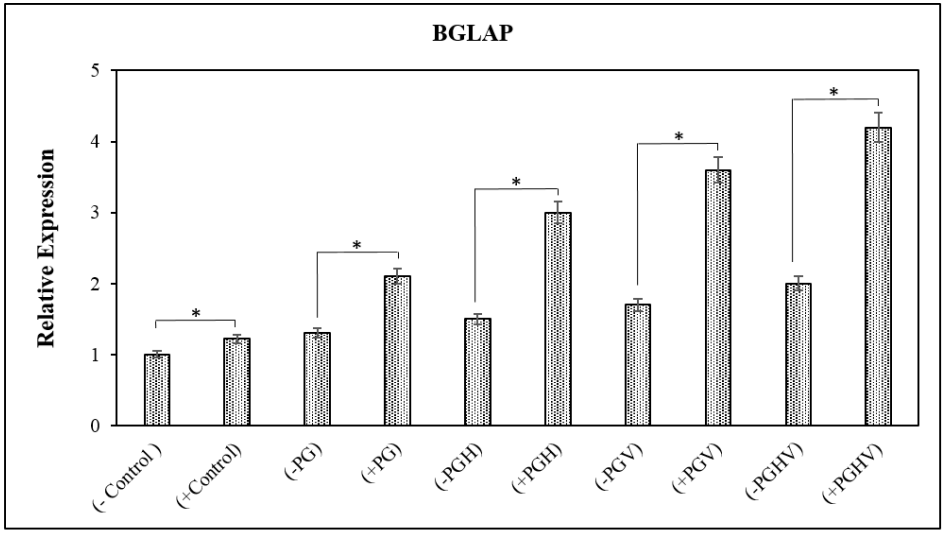
BGLAP
Relative Expression
0
1
2
3
4
5
*
(- Control)
(+Control)
(-PG)
(+PG)
(-PGH)
(+PGH)
(-PGV)
(+PGV)
(-PGHV)
(+PGHV)

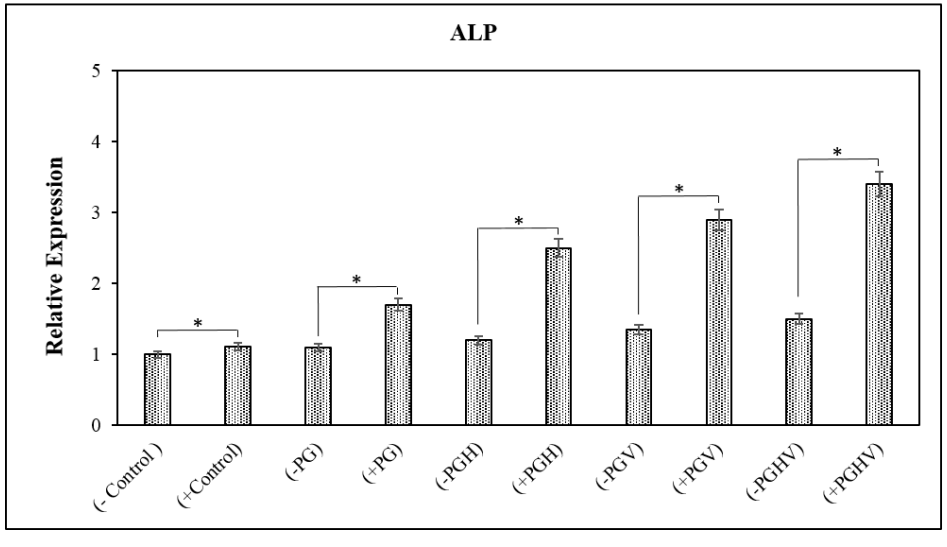
ALP
Relative Expression
0
1
2
3
4
5
*
(- Control)
(+Control)
(-PG)
(+PG)
(-PGH)
(+PGH)
(-PGV)
(+PGV)
(-PGHV)
(+PGHV)

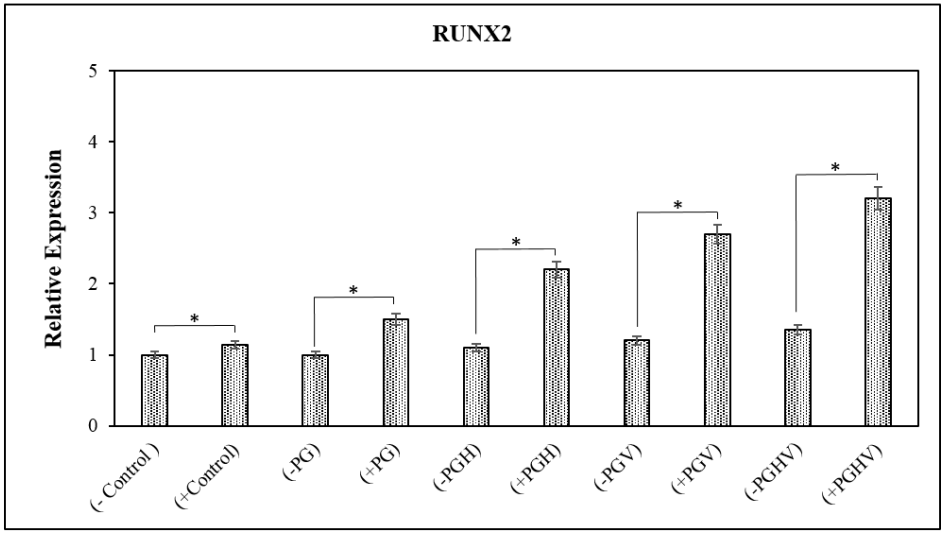
RUNX2
Relative Expression
0
1
2
3
4
5
*
(- Control)
(+Control)
(-PG)
(+PG)
(-PGH)
(+PGH)
(-PGV)
(+PGV)
(-PGHV)
(+PGHV)

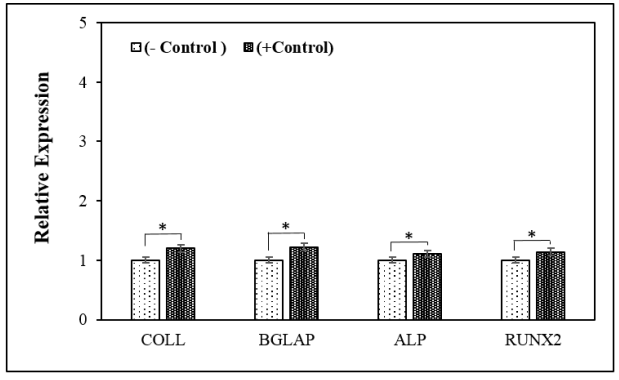
(- Control)
(+Control)
Relative Expression
0
1
2
3
4
5
COLL
BGLAP
ALP
RUNX2

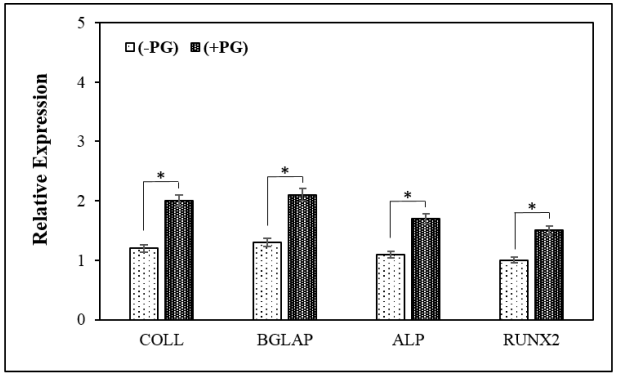
(-PG)
(+PG)
Relative Expression
0
1
2
3
4
5
COLL
BGLAP
ALP
RUNX2

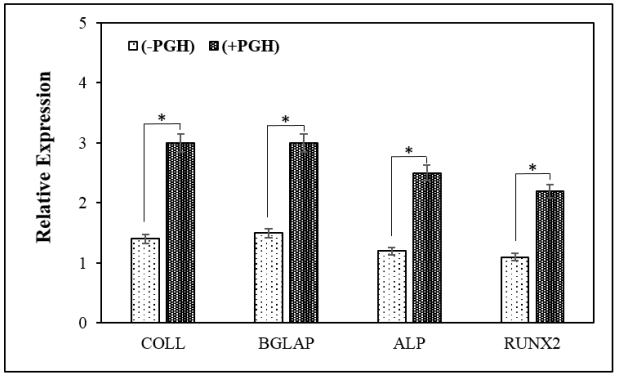
(-PGH)
(+PGH)
Relative Expression
0
1
2
3
4
5
COLL
BGLAP
ALP
RUNX2

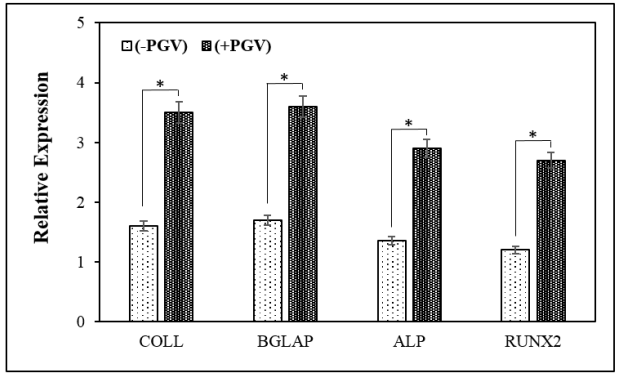
(-PGV)
(+PGV)
Relative Expression
0
1
2
3
4
5
COLL
BGLAP
ALP
RUNX2

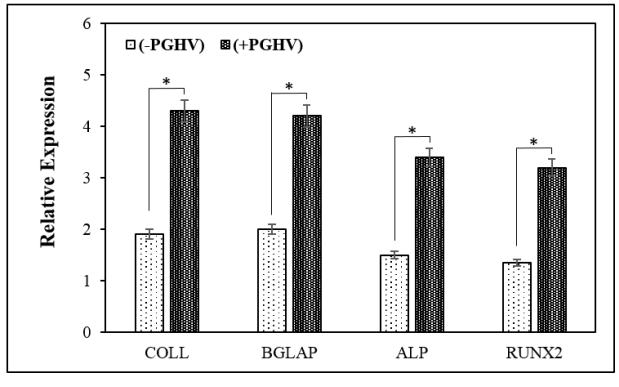
(-PGHV)
(+PGHV)
Relative Expression
0
1
2
3
4
5
6
COLL
BGLAP
ALP
RUNX2

Table 1: The sample code used in cell culture

Number	Sample Code	Sample Material
1	-control	cells free scaffold
2	-PG	PCL/Gel scaffold with cells
3	-PGH	PCL/Gel/nHA scaffold with cells
4	-PGV	PCL/Gel/Vit D3 scaffold with cells
5	-PGHV	PCL/Gel/nHA/Vit D3 scaffold with cells
6	+control	Negative control complemented with osteogenic factors consisting of β-glycerol phosphate, dexamethasone, ascorbic acid-2-phosphate (representing the +control)
7	+PG	PCL/Gel scaffold with cells
8	+PGH	PCL/Gel/nHA scaffold with cells
9	+PGV	PCL/Gel/Vit D3 scaffold with cells
10	+PGHV	PCL/Gel/nHA/Vit D3 scaffold with cells

(-) Cell culture medium, (+) Bone induction medium

Table 2: The sequence of primers used in RT-PCR

Primer of Osteogenic Genes	Sequence (5' → 3')	Scale (OD)	Number of Nucleotides
GAPDH-F	TTGAGGTCAATGAAGGGGTC	4	18
GAPDH-R	GAAGGTGAAGGTCGGAGTCA	4	18
COLL I-F	CCGTGACCTCAAGATGTG	4	18
COLL I-R	CCATACTCGAACTGGAATC	4	19
RUNX2-F	CGGAATGCCTCTGCTGTTATG	4	21
RUNX2-R	TGTCTGTGCCTTCTGGGTTC	4	20
ALP-F	TTGACCTCCTCGGAAGACA	4	19
ALP-R	GTAGTTGTTGTGAGCATAGTCC	4	22
BGLAP-F	TTGGACACAAAGGCTGCAC	4	19
BGLAP-R	CTCACACTCCTCGCCCTATT	4	20

Table 3: The fibers properties of PCL/Gel, PCL/Gel/nHA, PCL/Gel/Vit D3 and PCL/Gel/nHA/Vit D3 electrospun

Sample	Diameter (nm)	Pore Size (µm)	Porosity (%)
PCL/Gel	594 ± 83.15	8.21	82.19
PCL/Gel/nHA	631 ± 90.40	8.73	83.52
PCL/Gel/Vit D3	558 ± 66.21	8.15	82.02
PCL/Gel/nHA/Vit D3	622 ± 82.82	8.54	83.11